COMPARATIVE STUDY OF FINITE ELEMENT ANALYSIS AND GEOMETRICALLY EXACT BEAM ANALYSIS OF A COMPOSITE HELICOPTER BLADE

A THESIS SUBMITTED TO
THE GRADUATE SCHOOL OF NATURAL AND APPLIED SCIENCES
OF
MIDDLE EAST TECHNICAL UNIVERSITY

BY

MERYEM NİSA ATAÇ

IN PARTIAL FULFILLMENT OF THE REQUIREMENTS
FOR
THE DEGREE OF MASTER OF SCIENCE
IN
AEROSPACE ENGINEERING

JANUARY 2018

Approval of the thesis:

COMPARATIVE STUDY OF FINITE ELEMENT ANALYSIS AND GEOMETRICALLY EXACT BEAM ANALYSIS OF A COMPOSITE HELICOPTER BLADE

submitted by **MERYEM NİSA ATAÇ** in partial fulfillment of the requirements for the degree of **Master of Science in Aerospace Engineering Department, Middle East Technical University** by,

Prof. Dr. Gülbin Dural Ünver _____
Dean, Graduate School of **Natural and Applied Sciences**

Prof. Dr. Ozan Tekinalp _____
Head of Department, **Aerospace Engineering**

Prof. Dr. Altan Kayran _____
Supervisor, **Aerospace Engineering Department, METU**

Examining Committee Members:

Assoc. Prof. Dr. Demirkan Çöker
Aerospace Engineering Department, METU _____

Prof. Dr. Altan Kayran
Aerospace Engineering Department, METU _____

Assoc. Prof. Dr. Melin Şahin
Aerospace Engineering Department, METU _____

Assoc. Prof. Dr. Ferhat Akgül
Department of Engineering Sciences, METU _____

Prof. Dr. Kemal Levend Parnas
Department of Mechanical Engineering, TED University _____

Date: _____

I hereby declare that all information in this document has been obtained and presented in accordance with academic rules and ethical conduct. I also declare that, as required by these rules and conduct, I have fully cited and referenced all material and results that are not original to this work.

Name, Last Name: MERYEM NİSA ATAÇ

Signature :

ABSTRACT

COMPARATIVE STUDY OF FINITE ELEMENT ANALYSIS AND GEOMETRICALLY EXACT BEAM ANALYSIS OF A COMPOSITE HELICOPTER BLADE

Ataç, Meryem Nisa
M.S., Department of Aerospace Engineering
Supervisor : Prof. Dr. Altan Kayran

January 2018, 76 pages

In this master thesis, comparative study of the finite element analysis and geometrically exact beam analysis of a composite helicopter blade is performed. The objective of this study is to investigate the applicability of the geometrically exact beam analysis of the composite helicopter blade in predicting the structural response of the composite blade. To evaluate the structural response determined by the geometrically exact beam analysis of the composite blade, detailed finite element model of the blade is prepared and the structural response of two methods are compared for different static and transient load cases and dynamic analysis. Geometrically exact beam analysis utilizes variational asymptotic beam section analysis for the calculation of sectional stiffness and mass matrices, and general deformation of the blade for the static and transient load cases can be determined with high accuracy. Three dimensional stresses in the selected blade sections can also be determined via the stress recovery feature of the variational asymptotic beam section method. It is shown that the neutral axis,

shear center, still air natural frequency, static and transient displacement and static stress analysis results determined by the geometrically exact beam analysis match perfectly with the finite element analysis results for the rectangular section and airfoil section blade models studied. It is considered that especially for the structural design of the airfoil sections of the blade, which requires many re-analyses due to frequent design changes in the detailed design stage, geometrically exact beam analysis can replace finite element method which requires longer modelling times to reflect the design changes.

Keywords: helicopter blade, composite, finite element analysis, VABS, GEBT

ÖZ

KOMPOZİT HELİKOPTER KANAT YAPISININ SONLU ELEMANLAR METODU VE GEOMETRİK OLARAK KESİN KİRİŞ TEORİSİ KULLANILARAK YAPILMIŞ OLAN ANALİZLERİNİN KIYASLANMASI

Ataç, Meryem Nisa
Yüksek Lisans, Havacılık ve Uzay Mühendisliği Bölümü
Tez Yöneticisi : Prof. Dr. Altan Kayran

Ocak 2018 , 76 sayfa

Bu yüksek lisans tezinde, kompozit bir helikopter palinin yapısal analizleri sonlu eleman ve geometrik olarak kesin kiriş analiz (GEBT) metodu kullanılarak yapılmış ve bu iki analiz metodu kıyaslanmıştır. Bu çalışmanın amacı geometrik olarak kesin kiriş analiz metodunun; kompozit helikopter palin yapısal sonuçlarını ölçmedeki gücünü incelemektir. Geometrik olarak kesin kiriş analiz metodu kullanılarak elde edilen kompozit helikopter palinin yapısal tepkilerini değerlendirmek için palin detaylı sonlu elemanlar modeli hazırlanmıştır. Bu metotlar kullanılarak palin farklı yük koşulları altındaki statik, dinamik ve zamana bağlı analiz sonuçları karşılaştırılmıştır. Geometrik olarak kesin kiriş analizi; değişimsel asimtotik kiriş kesit analizinden (VABS) kesit katılık ve kütle matrislerini alarak statik ve zamana bağlı yük koşulları altındaki palin genel deformasyonunu yüksek çözünürlükle hesaplamaktadır. Değişimsel asimtotik kiriş kesit analizi metodunun gerilim iyileştirme özelliği sayesinde seçili pal kesitlerinde üç-boyutlu gerilim hesabı da yapılabilmektedir. Üzerinde çalışılan dikdörtgen ve pal kesitlerinde; geometrik olarak kesin kiriş analizi kullanılarak

elde edilen nötr eksen, kesme ekseni, doğal frekans, statik ve zamana bağlı deformasyon ve statik gerilim sonuçlarının sonlu elemanlar kullanılarak elde edilen sonuçlarla iyi örtüştüğü gösterilmiştir. Palin detaylı tasarım aşamasında tasarımın sürekli değişmesinden kaynaklı çok fazla analiz gerekmektedir. Özellikle bu tasarım aşamasında, pal kesitlerinin yapısal tasarımında geometrik olarak kesin kiriş analiz metodu kullanılarak, tasarım değişikliğine yansıması çok daha fazla zaman alacak olan sonlu elemanlar metodu kullanımına kıyasla hatrısayılır zaman tasarrufu yapılabilmektedir.

Anahtar Kelimeler: helikopter pali, kompozit, sonlu elemanlar analizi, VABS, GEBT

To my family and people who are reading this page

ACKNOWLEDGMENTS

First of all, I would like to express my deepest appreciation to my supervisor Professor Altan Kayran for his supervision, guidance, and valuable support. It was a great honor to work with him for the last five years and our cooperation influenced my academical and work life highly.

I would also like to thank to Gökhan Tursun, who was our chief engineer of the composite helicopter structures when I was working in TAI, for encouragement to me for this research.

I am also grateful to my husband, Ali Osman Ataç, who has given all my motivation to complete my thesis. When the tasks seemed very hard to be handled, he was the one encouraged me. Thank you for being by my side.

Finally, I am really thankful to my family for their everlasting patience and support throughout my years of study. This accomplishment would not have been possible without them. Thank you.

TABLE OF CONTENTS

LIST OF TABLES

TABLES

LIST OF FIGURES

FIGURES

LIST OF ABBREVIATIONS

BC	Boundary Condition
DLL	Dynamic Link Libraries
dof	Degree of Freedom
FA	Feathering Axis
FE	Finite Element
FEA	Finite Element Analysis
FEM	Finite Element Method
GEBT	Geometrically Exact Beam Theory
NA	Neutral Axis
RPM	Revolutions per Minute
SC	Shear Center
STA	Station
VABS	Variational Asymptotic Beam Sectional Analysis
1D	One-Dimensional
2D	Two-Dimensional
3D	Three-Dimensional
E	Young's Modulus
G	Shear Modulus
ν	Poisson's Ratio
ρ	Density

CHAPTER 1

INTRODUCTION

In the design process of helicopter, the structural analysis of the blades constitutes one of the most important tasks. Since a helicopter blade has a long span in proportion to chord and thickness, it is named as a slender body.

In the production of the helicopter blades, use of the composite materials has increasing demand. Composite materials have higher stiffness-to-weight ratio, superior fatigue characteristics, and better corrosion resistance compared to metals. These are the main reasons of choosing composite materials over metals for the construction of helicopter blade.

To analyze a slender composite structure like a helicopter or a wind turbine blade, mostly finite element methods have been used since many experiments have been done to validate the finite element approach. In the preliminary design stage of helicopter blades many re-analyses have to be performed. Performing finite element analysis of helicopter blades is costly because of the complex structure of the helicopter blade. Therefore, in the preliminary design stage, get sufficiently reasonable results, recently, cross-sectional analysis coupled with 1D beam analysis have been preferred. By means of cross-sectional analysis, sectional beam properties, such as mass and stiffness, of complex blade cross-sections are determined. Sectional properties are then transferred to the beam analysis to perform the analysis of slender structures such as helicopter blades with complex cross-sections.

In this study, for the two-dimensional cross-section analysis, Variational Asymptotic Beam Sectional Analysis (VABS)[1] is used together with the Geometrically Exact Beam Theory (GEBT)[2]. Geometrically exact beam theory handles geometric nonlinearities of one-dimensional slender structures such as helicopter blades modeled as beams. VABS also needs a pre-processor for the modeling of the blade cross-sections

in 2D. In the present study, Pre-VABS[3] is used as the pre-processor of VABS. For the 3D model of the helicopter blade, finite element model is used and as the finite element tool, MSC. PATRAN and NASTRAN are used as pre and post processors, respectively. A summary of the process of generating the beam model of the complex helicopter blade is shown in Figure - 1.1. When the 3D finite element model of the blade is prepared, the number of degrees of freedom to use can be very high depending on the complexity of the blade structure. On the other hand, in the two step approach, 2D sectional analysis are done in certain number of sections, usually between 10-20, to determine the beam section properties of the blade. These properties are then transferred to the 1D beam model which requires far less number of degrees of freedom compared to the 3D finite element model. The two-step approach is especially very useful in performing many re-analyses during the preliminary design stage of the helicopter blade, or static and dynamic aeroelastic analysis of the blades. With the two-step approach, computational cost of the blade analysis is significantly reduced.

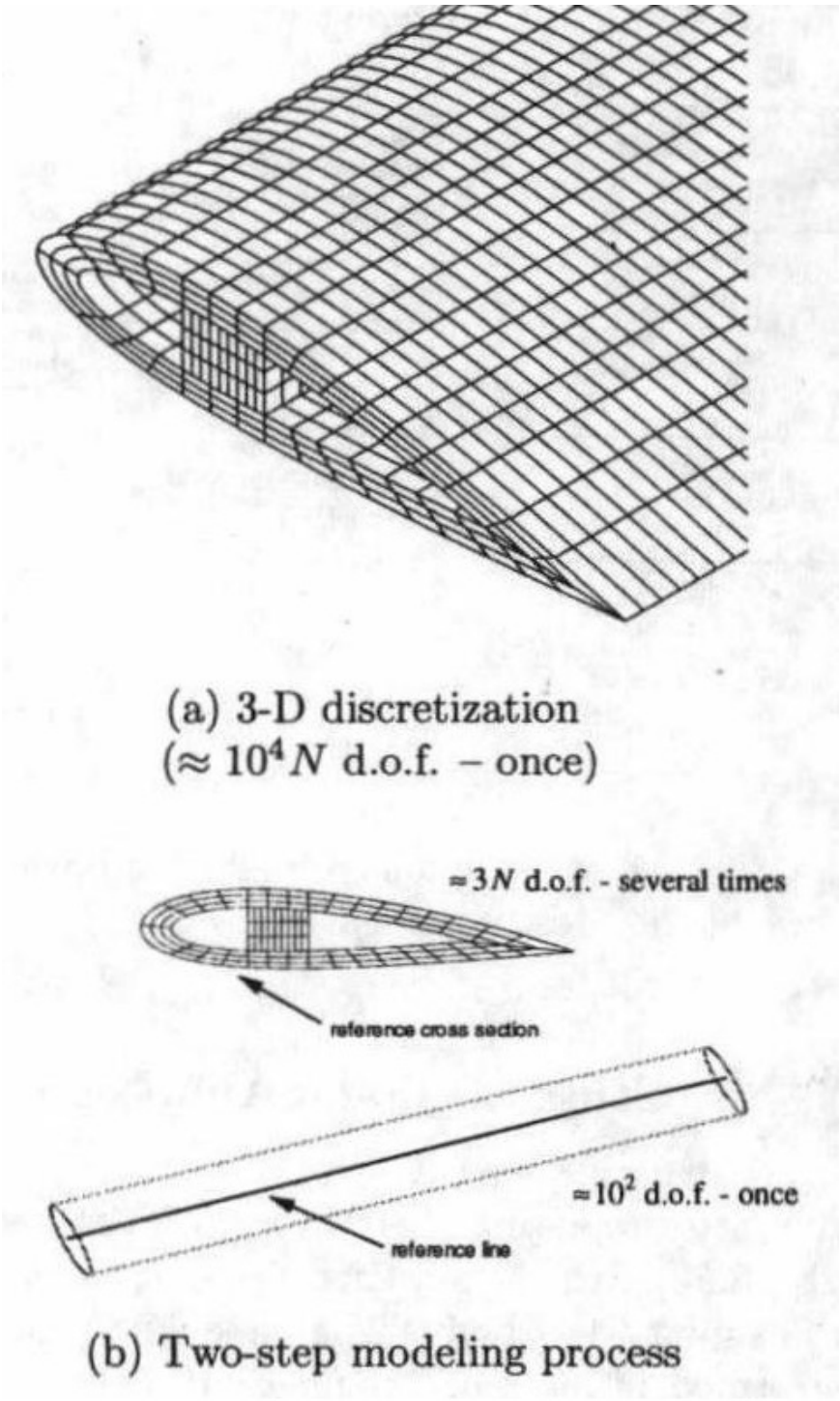

Figure 1.1: Schematic of the discretization process of a rotor blade[4]

The utilized tools; PreVABS, VABS and GEBT are described briefly in the following paragraphs.

For airfoil like structures, the easiest way to prepare the finite element mesh necessary for VABS is to use PreVABS which is the preprocessor of VABS, as mentioned before. In the preparation of the blade sections in Pre-VABS, the external profile should be indicated by nodes as described in the Pre-VABS manual[3]. The blade cross-section is then meshed and by giving composite layup information and material properties as input to the PreVABS program, the airfoil section with all properties defined is obtained.

By VABS, various effects; such as warping, recovery of stress, trapeze effect, curvature effect, etc. can be taken into account. Depending on the purpose of the analysis, these effects can be included in the VABS analysis. For detailed information, Yu[1] can be a guide. According to the selected influences, corresponding output are obtained.

To get the stresses, stress recovery selection is made and the sectional loads are introduced, and VABS is rerun. By this way, three dimensional strains and stresses are available in the sections of the blades in different coordinate systems.

GEBT is the abbrevation of Geometrically Exact Beam Theory. The theory is developed by Prof. Hodges of Georgia Institute of Technology[2]. There is a tool with the same name of the theory.

In GEBT, equations of motion are derived by a mixed variational formulation[5]. All geometric nonlinearities caused by large deflections and rotations can be handled as long as there is no material nonlinearities. In other words, GEBT uses small strain assumption. Geometrically exact refers to the fact that the finite rotation of the cross-sectional frame is treated exactly, without small-angle assumptions. The term geometrically exact means that the displacement of the reference line and the variation of the orientation of the cross-sectional reference frame are represented exactly. For GEBT analysis, the input file requires the information that comes from VABS analysis such as mass and stiffness matrices of the selected cross-sections. Moreover, beam modeling of the structure in the spanwise direction is performed via the definitions made in the input file. By the GEBT tool, both linear and nonlinear static, modal and dynamic analyses can be performed for beam like structures. At the end of the analysis, displacement, rotation, cross-sectional forces and moments for each node

definition, linear and angular momenta, eigenvalues and eigenvectors can be obtained depending on the type of the analysis[2].

1.1 Motivation of the Study

The objective of this thesis is to investigate the applicability of the geometrically exact beam analysis of the composite helicopter blade in predicting the structural response of the real composite blade. Helicopter blades work in extremely dynamic environment due to the flexibility of the rotary blades and articulation. Accurate blade models and faster analyses are needed in order to expedite the preliminary design process of helicopter blades. To analyze a slender composite structure like a helicopter or a wind turbine blade, mostly finite element methods have been used since many experiments have been done to validate these tools until now. Performing three-dimensional finite element analyses for helicopter blades requires large models and it is costly to implement finite element analysis in every design iteration during the preliminary design stage of a helicopter blade which requires many repeated analyses to coincide certain critical axes with each other, such as aerodynamic center, mass center and shear center of blade sections. In order to save time and get sufficiently reasonable results, recently, accurate 1D beam models, such as GEBT tool, complemented by 2D cross-sectional analysis, such as VABS, have been used in the analysis of slender structures such as helicopter blades. By one-dimensional beam analysis, various types of analyses can be performed such as static, eigenvalue and transient, in other words, in the preliminary design process, helicopter blade can be analyzed very quickly. Thus, design optimizations can be done before it is too late to make changes in the design. It should be noted that combined 2D cross-sectional and 1D beam analyses for real helicopter blades have been performed less than the analysis of slender beam-like structures with simple cross-sections such as rectangular, circular etc. With the current study, it aimed to investigate the applicability of the combined 2D cross-sectional and 1D beam analysis of composite helicopter blade with realistic lamination scheme. For this purpose, results obtained by the combined 2D cross-sectional and 1D beam analysis of composite helicopter blade are compared with the 3D finite element analysis results of the blade for different analysis types such as static and transient loading,

modal analysis for the rotating and stationary blades.

1.2 Scope

The thesis is organized in five chapters and brief description of the chapters are given below.

Chapter 1 includes introduction, literature survey and objective of the study.

In Chapter 2, theory of the cross-sectional analysis is given. The procedure of performing the cross-sectional analyses is presented in detail. Then, the variational asymptotic beam section method (VABS)[1] and the geometrically exact beam theory (GEBT)[2], are explained concisely. At the end of this chapter, the advantages and disadvantages of using the reduced order models utilizing the combination of VABS-GEBT against the finite element method are listed.

In Chapter 3, the beam-blade models are introduced. There are three different models used in this study. These are; composite rectangular cross-section, the isotropic (Aluminum) and the composite airfoil blade models. The details of the finite element and the cross-sectional analysis models are described in this chapter. For each finite element model; 3D finite element model, material, boundary conditions and load application points are shown by the relevant figures. Furthermore, for each VABS-GEBT model; cross-section, mesh, and also the Timoshenko stiffness matrix calculated by the VABS are presented.

Chapter 4 gives the results of the blade models introduced in the previous chapter. The results of the static, modal and transient analyses obtained by the finite element analysis (FEA) and the GEBT-VABS combination are compared. Furthermore, the effect of the geometric nonlinearity is studied through for static and transient analyses problems. For each case, the load applied is highlighted in the corresponding subsection. The results are presented by figures and tables.

In the last chapter, conclusions are given by first emphasizing the the purpose of the study. The conclusions drawn from the results obtained from the comparison studies performed by the finite element analysis and geometrically exact beam analysis are summarized. Besides, future works are suggested.

CHAPTER 2

LITERATURE SURVEY

In this chapter, examples are given from the two-level analyses involving combination of cross-sectional analysis and the 1D beam analysis.

In the study of Yu et al.[6], different tools developed for determination of the structural properties of wind turbine blades are compared. One of the examples demonstrated in this study is a multi-ply composite pipe. The model is described in Figure - 2.1 and its stiffness properties calculated by these tools with their percentage differences compared to the Saint Venant Beam Theory (SVBT) results are shown in Table - 2.1. In the study of Giavott et al.[7], Saint Venant Beam Theory is improved and SVBT refers to the computer tool that uses this theory. In this tool, only Timoshenko stiffness matrix is obtained.

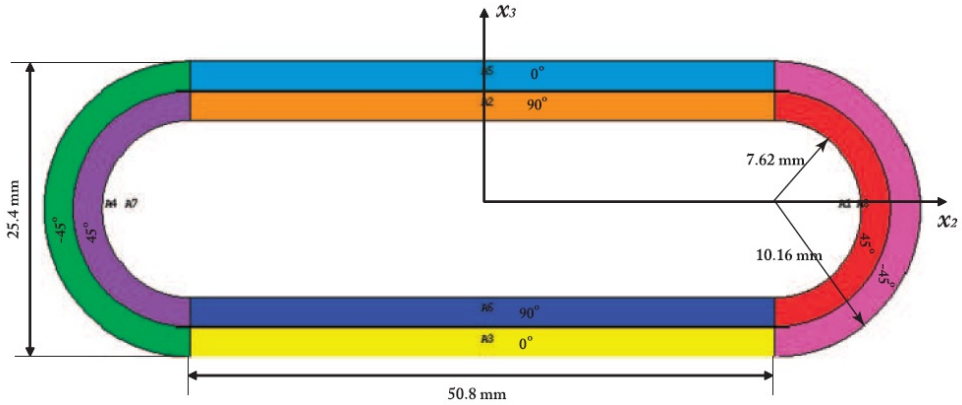

Figure 2.1: Schematic model of the multiply composite pipe[6].

Table 2.1: Sectional properties comparison of the composite elliptical pipe[6].

Variables	EI_{22}	EI_{33}	GJ	EA	S_{12}
PreComp	7.074E+03	4.857E+04	8.628E+03	7.833E+07	-1.205E-02
VABS	5.402E+03	1.547E+04	1.972E+03	4.621E+07	1.111E+04
FAROB	6.182E+03	2.297E+04	4.240E+03	/	/
CROSTAB	6.694E+03	4.012E+04	1.500E+01	7.000E+07	0.000E+00
SVBT	5.402E+03	1.547E+04	1.972E+03	4.621E+07	1.112E+04
percentage diff. (PreComp)	30.950	214.005	337.447	69.499	100
percentage diff. (VABS)	0.001	0.003	0.044	0.0004	0.172
percentage diff. (FAROB)	14.429	48.485	114.974	/	/
percentage diff. (CROSTAB)	23.906	159.363	99.240	51.465	100

It can be pointed out that VABS gives reasonable results compared to the other computer programs.

In the study of Wang et al.[8], static, eigenvalue and dynamic analyses of a wind turbine system is performed by taking into account the geometrical nonlinear effects. For this purpose, Geometrically Exact Beam Theory (GEBT) is used in this study. Here one example is given on dynamic analysis of an isotropic joint beam under sinusoidal vertical load applied on the joint. The model shown in Figure - 2.2 is analyzed by ANSYS and GEBT. The comparison of the natural frequencies is given in Table - 2.2.

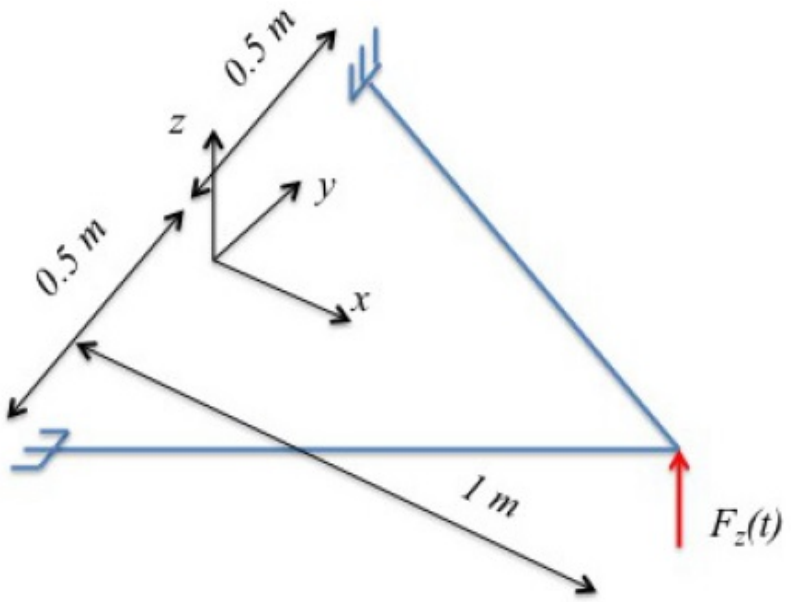

Figure 2.2: Undeformed beam assembly model[8].

Table 2.2: Comparison of natural frequency results of joint beam[8].

	1	2	3	4	5
GEBT	35.23	171.02	215.87	275.05	407.2
ANSYS	35.12	169.83	212.53	273.34	403.53
Percent Difference	0.17	0.70	1.57	0.63	0.91

In the study of Yu et al.[9], thin walled composite beams are analyzed by VABS and ABAQUS. For the isotropic and the anisotropic I-beam, axial stress results of VABS and ABAQUS are presented in Figure - 2.3, Figure - 2.4, Figure - 2.5, and Figure - 2.6. In the paper, it is pointed out that usage of different visualization tools is the reason of dissimilarities in the figure; however, correlation is good.

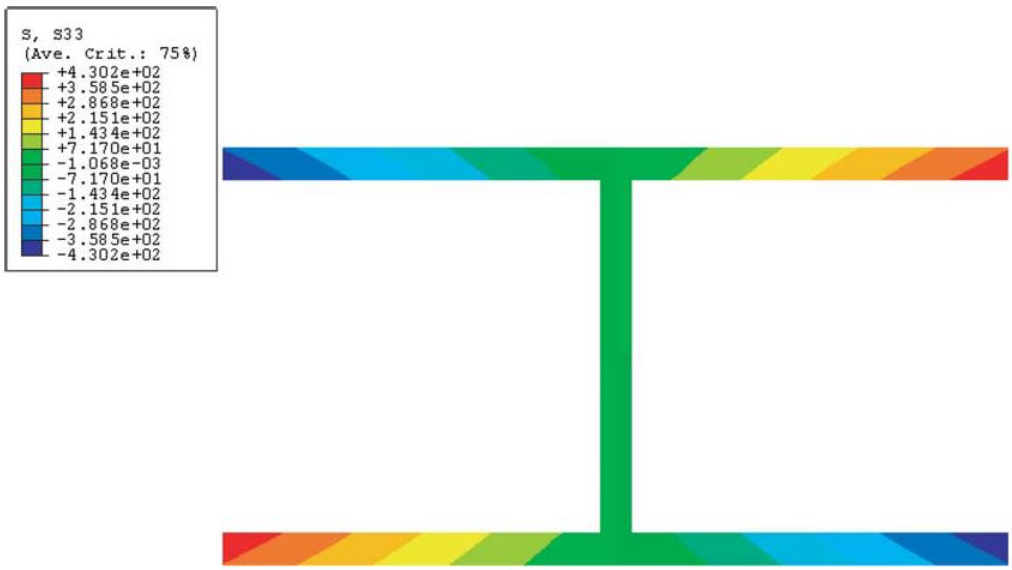

Figure 2.3: Axial stress result of the isotropic I-beam from ABAQUS[9].

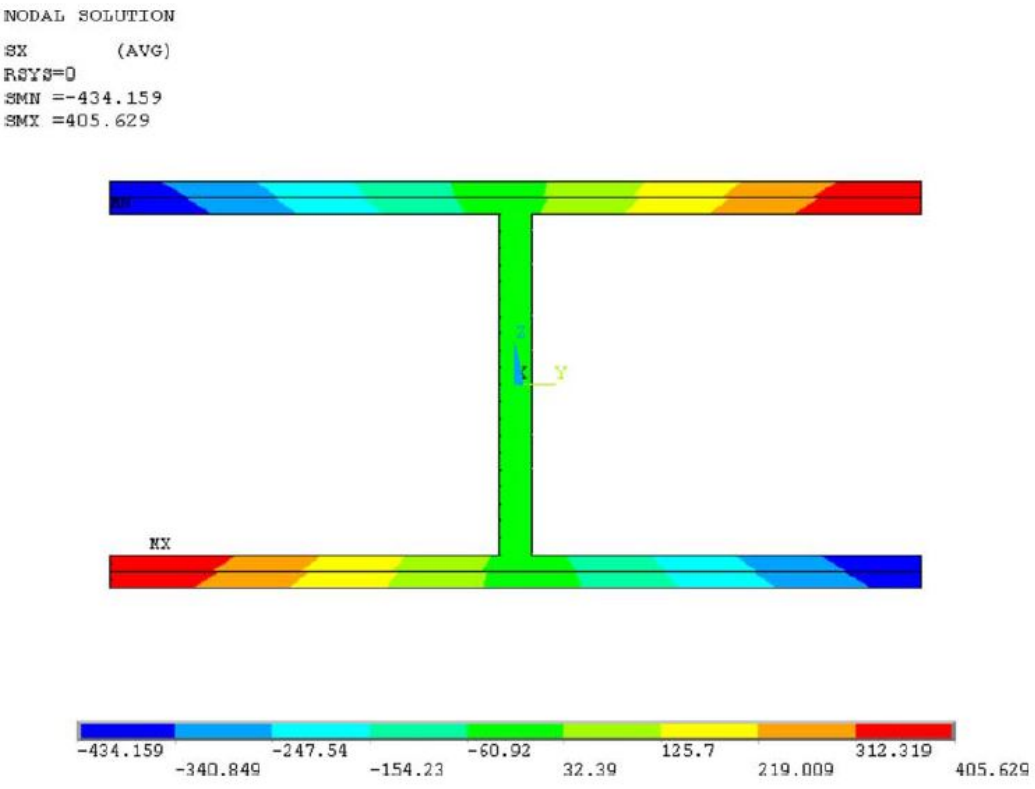

Figure 2.4: Axial stress result of the isotropic I-beam from VABS[9].

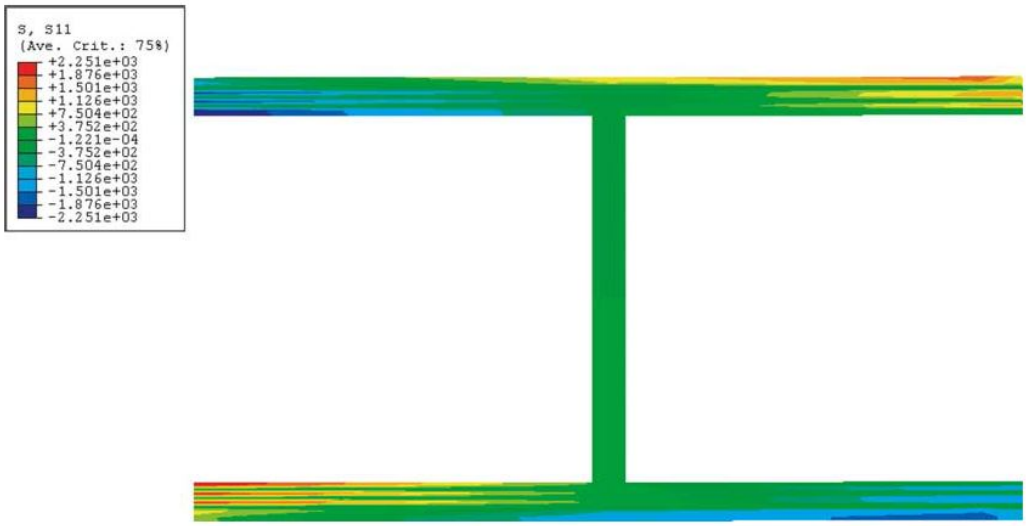

Figure 2.5: Axial stress result of the anisotropic I-beam from ABAQUS[9].

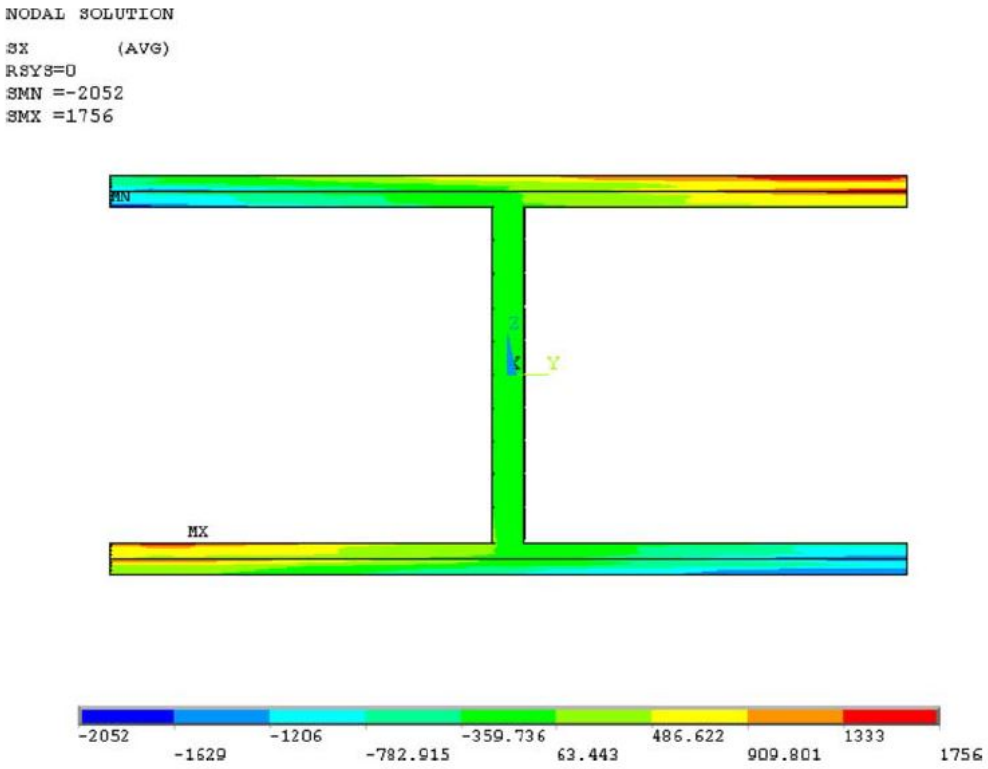

Figure 2.6: Axial stress result of the anisotropic I-beam from VABS[9].

In another study[10], generalized Timoshenko theory of VABS is validated numerically and analytically by some demonstrations. In one of the studies, a rectangular cross-section composite beam is analyzed. The material information and the schematic of the rectangular cross-section are given in Table - 2.3 and Figure - 2.7, respectively. It is indicated that there are total of 80 plies in the composite layup.

Table 2.3: Material properties of the rectangular cross-section beam[10].

Layup:	$[(-45/+45/0/90)_{10}]_s$
Material Properties:	$E_l = 20.59 \times 10^6 psi$
	$E_t = 1.42 \times 10^6 psi$
	$G_{lt} = G_{tn} = 8.7 \times 10^5 psi$
	$\nu_{lt} = \nu_{tn} = 0.42$
	$\rho = 0.057 lb.sec^2/in.^4$

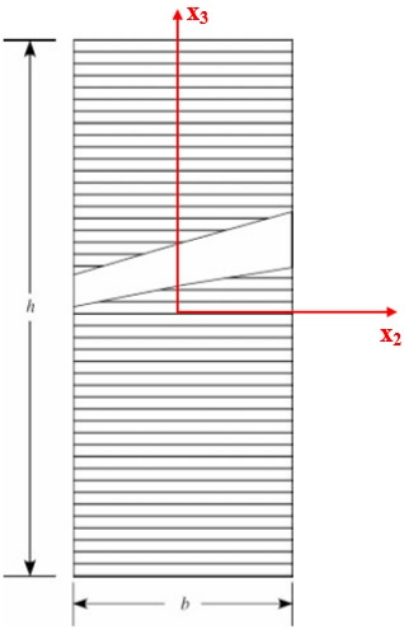

Figure 2.7: Rectangular beam cross-section[10].

The beam is fixed at one end and a shear force of 3 lb in the vertical direction is applied in the other end. The stresses at the mid-span at different locations are calculated by VABS and ANSYS. It is noted that although ANSYS requires about one hour to carry out this analysis, VABS requires less than two seconds. The variation of the

shear stress components along the thickness of the beam are shown in Figure - 2.8 and Figure - 2.9. It is seen that the results of the two programs are in very good agreement.

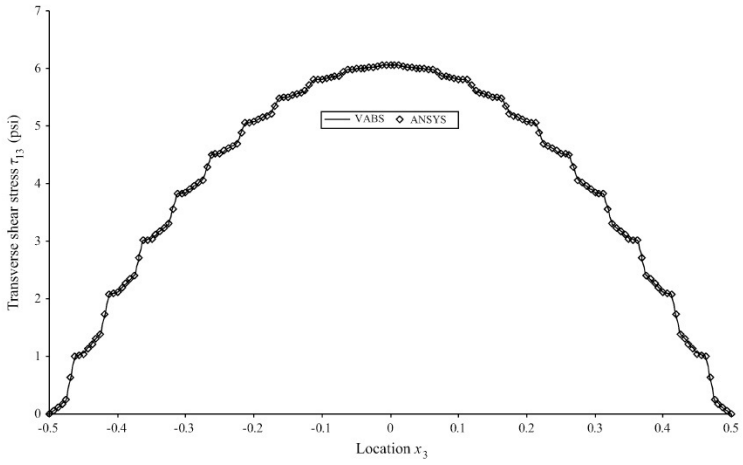

Figure 2.8: Shear stress component τ_{13} in the rectangular cross-section at mid-span and $x_2 = 0$[10].

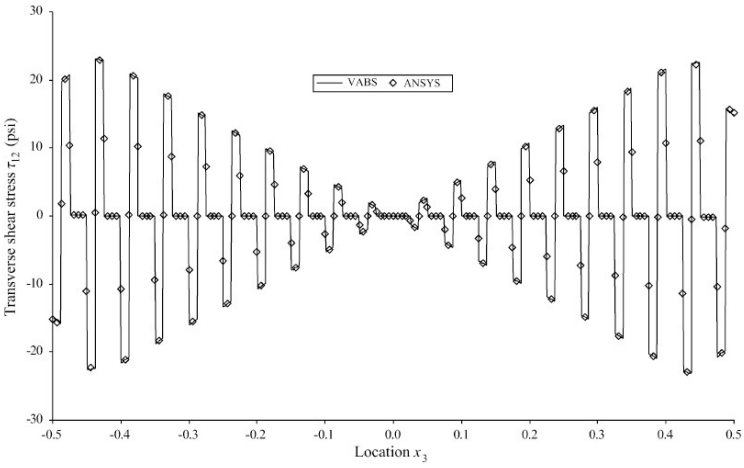

Figure 2.9: Shear stress component τ_{12} in the rectangular cross-section at mid-span and $x_2 = 0$[10].

In the study of Yu et al.[11], various validation demonstrations of GEBT are performed. In one of these validation studies, the analysis capability of GEBT for a rotating beam is presented. It is a swept tip aluminum beam which is used in the study of Hodges et al.[12]. A simple schematic of the beam is shown in Figure - 2.10. The width of the beam is 1" and the thickness is 0.063". The center of rotation of the

beam is point-O and the rotation axis is a_3 as shown in Figure - 2.10. There is 2.5" distance between the rotating center of rotation and the root of the beam. The length of the un-swept part of the beam is 31.5" whereas it is 6" for the swept part. The material properties of the rotating aluminum beam are given in Table - 2.4.

Figure 2.10: Rotating Aluminum beam with a swept tip[11].

Table 2.4: Aluminum material properties of the rotating beam[11].

$E = 1.06 \times 10^7 [lb/in^2]$
$\nu = 0.325$
$\rho = 2.51 \times 10^{-4} [lb.sec^2/in^4]$

The natural frequency results of the 1st, 2nd and 3rd bending modes and coupled torsion-bending mode are plotted for various rotating speeds and sweep angles in Figure - 2.11, Figure - 2.12, Figure - 2.13, and Figure - 2.14, respectively. In addition to natural frequency results of GEBT, experimental data provided by the study, Epps and Chandra[13], and numerical results provided by Hodges et al.[12] are also plotted in the graphs.

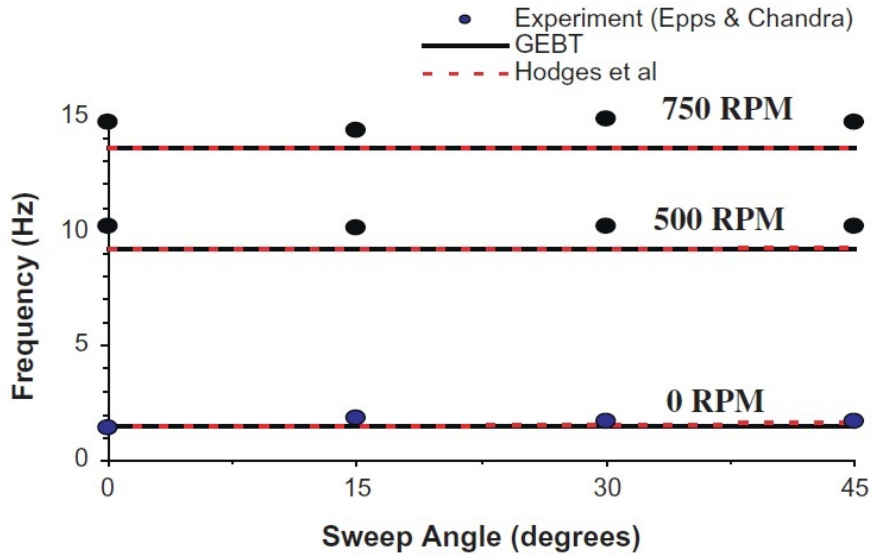

Figure 2.11: Frequency of the 1st-bending mode versus sweep angle and rotating speeds[11].

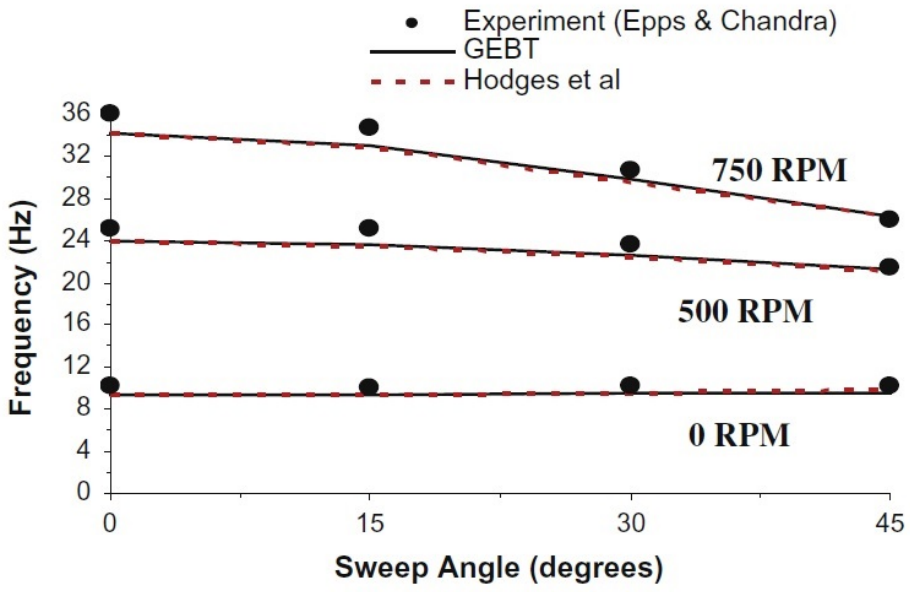

Figure 2.12: Frequency of the 2nd-bending mode versus sweep angle and rotating speeds[11].

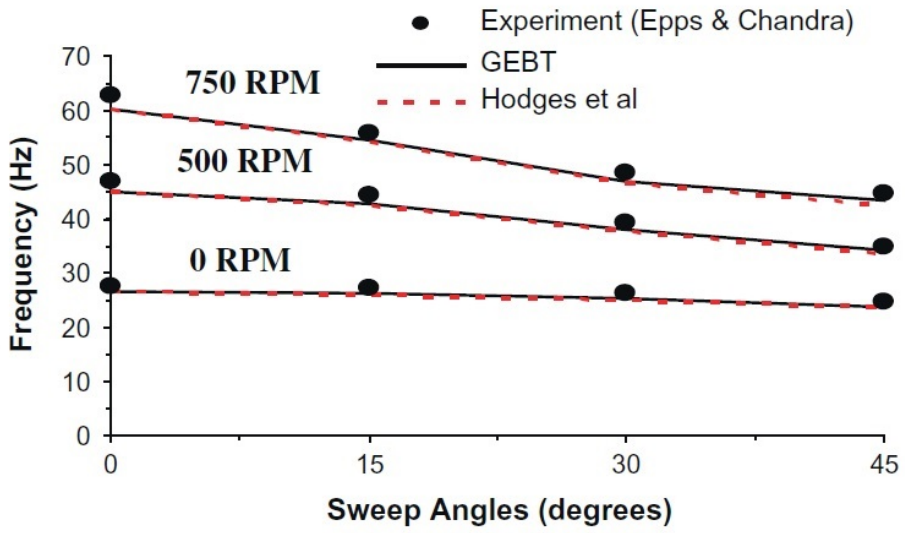

Figure 2.13: Frequency of the 3rd-bending mode versus sweep angle and rotating speeds[11].

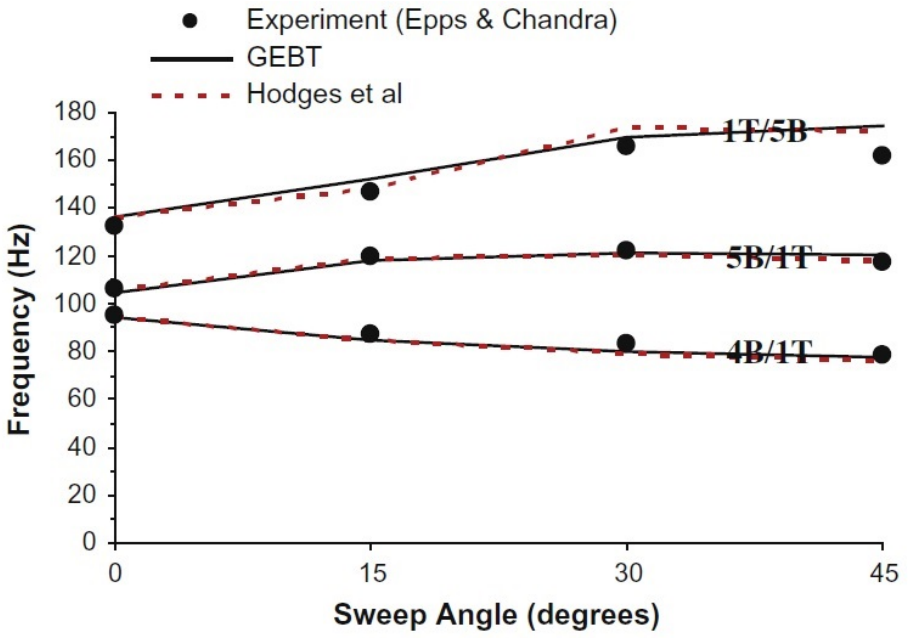

Figure 2.14: Frequency of coupled torsion-bending modes versus sweep angle at 750 rpm[11].

From these plots, it can be concluded that the results of GEBT are in good agreement with experimental and numerical results.

From these studies, it can be said that, in the static and dynamic analyses of a structural model, using VABS and GEBT together gives reasonable results compared to the analytical, experimental and finite element methods.

CHAPTER 3

THEORY OF CROSS-SECTIONAL ANALYSIS

3.1 Methodology of the Cross-Sectional Analysis

There are many studies done on the cross-sectional analysis of beam sections and VABS is one of the most accepted method used in the literature as mentioned before. To obtain the stiffness and mass matrices, shear center and other necessary outputs by the variational asymptotic beam section (VABS) method, there are some steps to be followed. This procedure is described in Figure - 3.1.

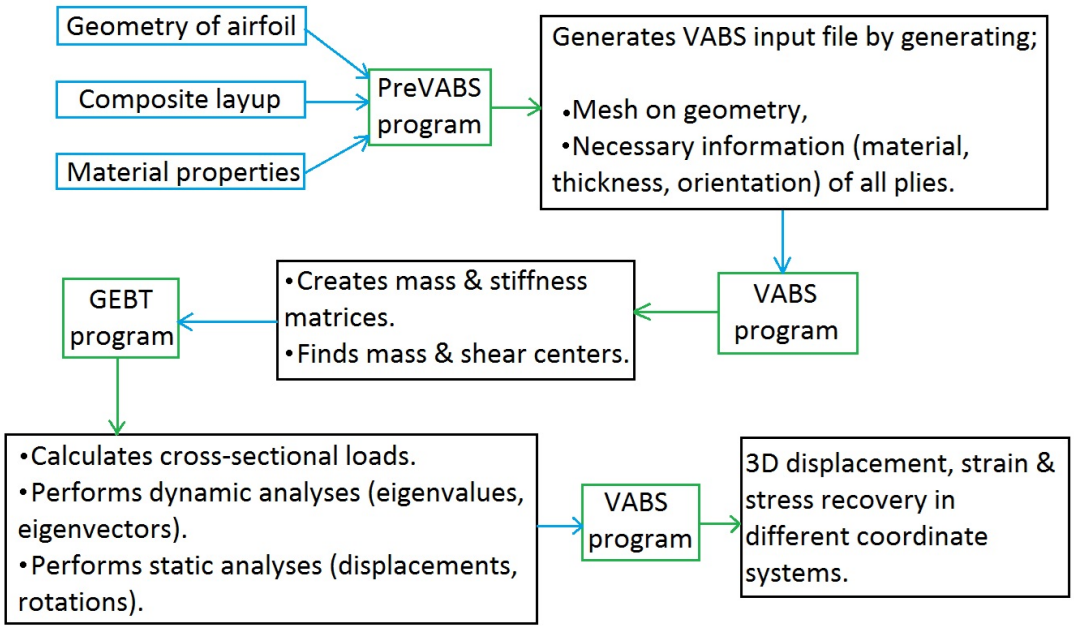

Figure 3.1: Procedure of the cross-sectional analysis by VABS and the subsequent stress recovery.

It is seen in Figure - 3.1 that, for cross-sectional analysis of beam sections firstly, VABS input file should be prepared. If the geometry is in the shape of an airfoil,

PreVABS[3], which is the preprocessor of VABS[1], is used for this purpose. PreVABS essentially generates a two-dimensional mesh in the cross-section of the airfoil shapes and prepares the input file necessary for VABS analysis. In this respect, PreVABS requires the geometric data of the airfoil used in the blade, material properties and composite layups of the sections. These data are given as input to PreVABS in different files. In the meshing procedure, PreVABS generates a single element per ply and VABS input file is created. Although PreVABS has some restrictions, it is very easy way to get the layered meshes compared to the finite element analysis. The selected cross-section can be analyzed by running the executable file of VABS. Secondly, by modeling the whole blade as a beam in the geometrically exact beam theory (GEBT) tool, loads acting on the particular section that is studied are determined. In addition, static and dynamic analyses of the blade can be performed by GEBT. To get the stresses, the last step is to rerun VABS by giving the sectional loads in the VABS input file for stress recovery.
The theory behind VABS and GEBT are described briefly in the following sections.

3.2 Theory of VABS

Various beam theories are used in the Variational Asymptotic Beam Sectional Analysis (VABS) tool[1]. VABS uses the Variational Asymptotic Method (VAM). In the thesis of Yu[14], VAM is defined as not only an asymptotic -which holds for kinematic assumptions- but also a variational method -holds for mathematically systematic -. A nonlinear 3D elasticity problem can be splitted into a linear problem for less significant dimensions and nonlinear problem for the more significant ones. Variational Asymptotic Method can be illustrated by a beam problem. By VAM, the problem decouples into a 2D linear cross-section analysis and 1D nonlinear beam analysis along the reference line.
By VABS, an arbitrary cross-section is analyzed in order to get all required information about the beam sections.

In terms of mass per unit length, 6×6 mass matrix and the second distributed mass moments of inertia about all axes are calculated. From the mass matrix, the cross-

sectional mass center, the principal mass moment of inertia, and the inertia principal axes are also found for the cross-section[1].

For the classical stiffness model, 4×4 stiffness matrix is constructed. For the Timoshenko model, 6×6 stiffness matrix is calculated. Moreover, the location of neutral axis and the shear center are also computed.
The shown coordinate system in Figure - 3.2 is used in VABS. According to this, the coordinate along the span is x_1 which points from root to tip, x_2 points from the leading edge to the trailing edge, and x_3 is determined by the right-hand rule. The origin of the local coordinate of the cross-section, x_2 and x_3 can be selected as any point on the cross-section.

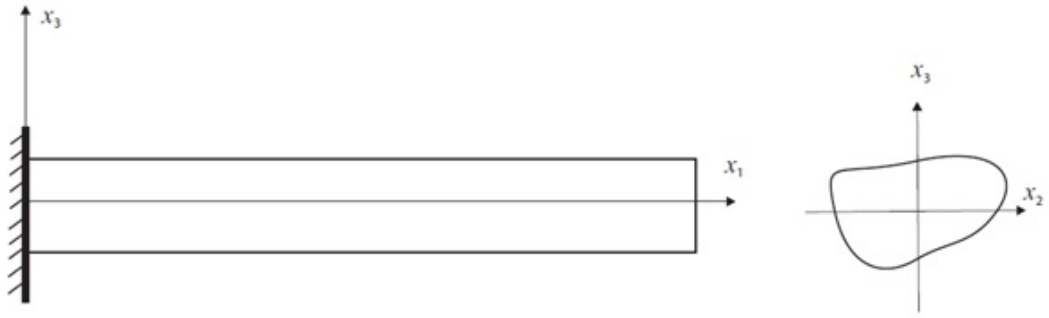

Figure 3.2: VABS beam coordinate system[1].

If there is an initial twist or taper in the model, they should be specified. For example, when the analyzed structure is a swept wing, the obliqueness, which is the angle between x_1 and the plane x_2 - x_3, should be given as input.
In the VABS mesh, the order of the nodes is in the counterclockwise direction which is shown for triangular and quadrilateral elements at the left side of Figure - 3.3 and Figure - 3.4, respectively.
The 3D displacements are calculated at the nodes of the elements in the beam coordinate system. However, 3D strains and stresses are calculated at the Gaussian integration points of the elements which are shown for triangular and quadrilateral elements at the right side of Figure - 3.3 and Figure - 3.4, respectively. In Figure - 3.3 and Figure - 3.4, the red points denote the Gauss points for linear and the green ones denote the Gauss points for quadratic elements. In VABS, strains and stresses are evaluated at the Gauss points in beam and material coordinate systems.

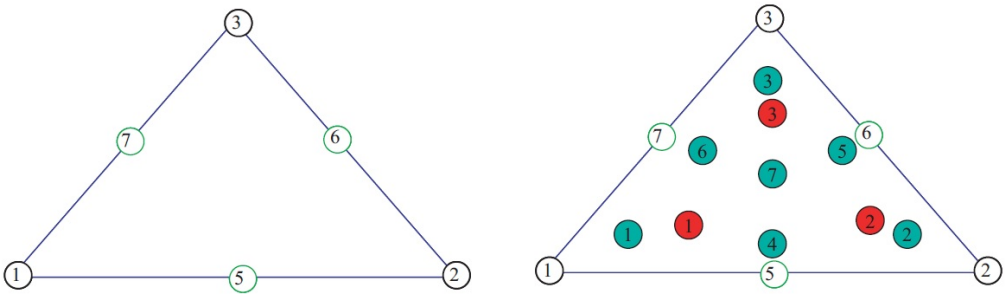

Figure 3.3: Node numbering and Gauss points of the triangular element in VABS[1].

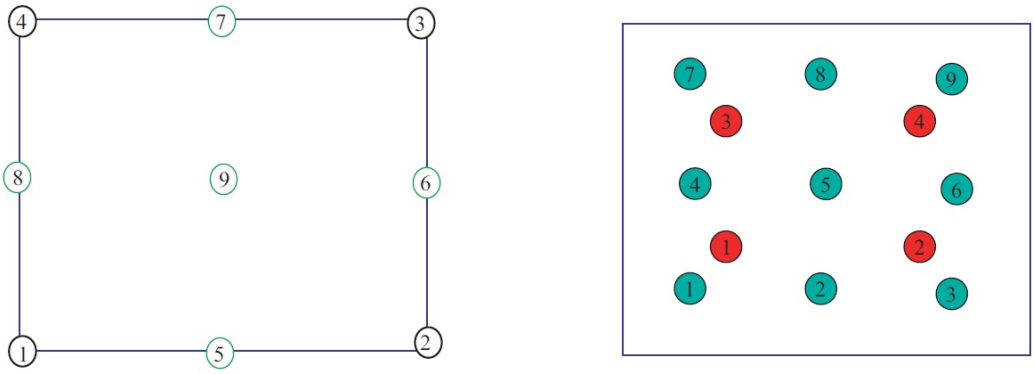

Figure 3.4: Node numbering and Gauss points of the quadrilateral element in VABS[1].

The beam coordinate system is to define the geometry, and the material coordinate system is for the definition of material properties. In Figure - 3.5, the relation between the beam (x_1, x_2, x_3), material (e_1, e_2, e_3), and ply plane (y_1, y_2, y_3) coordinate systems are shown. It is seen that by rotating the global x_1-x_2-x_3 by θ_1 $(0 \leq \theta_1 \leq 360)$ degrees in the right-hand sense about the x_1 axis, ply plane axis (y_1, y_2, y_3) is obtained. And, rotating the y axis by θ_3 $(-90 \leq \theta_3 \leq 90)$ degrees in the right-hand sense about the y_3 axis, the material coordinate system (e_i) is obtained. The range of θ_3 is consistent with the definition of the composite material orientation.

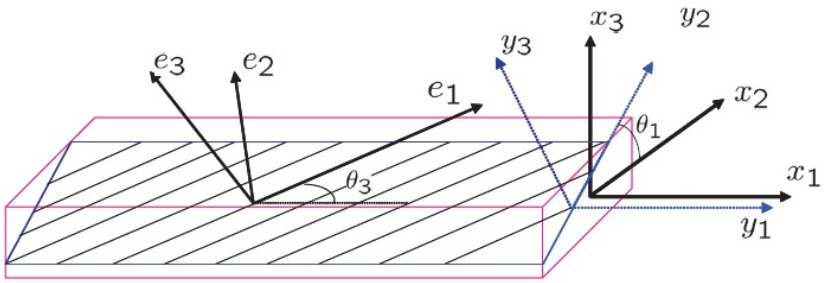

Figure 3.5: VABS Layup Convention[1].

VABS layup convention for a box beam is shown in Figure - 3.6. In the box-beam section, the respective coordinates are shown. Looking into the angle between x_2 & y_2, it can be indicated that for the upper wall θ_1 is $0°$, for the left wall it is $90°$, for the lower wall $180°$, and for the right wall $270°$. The stacking sequence is often given as input from innermost layer to the outermost layer for each wall.

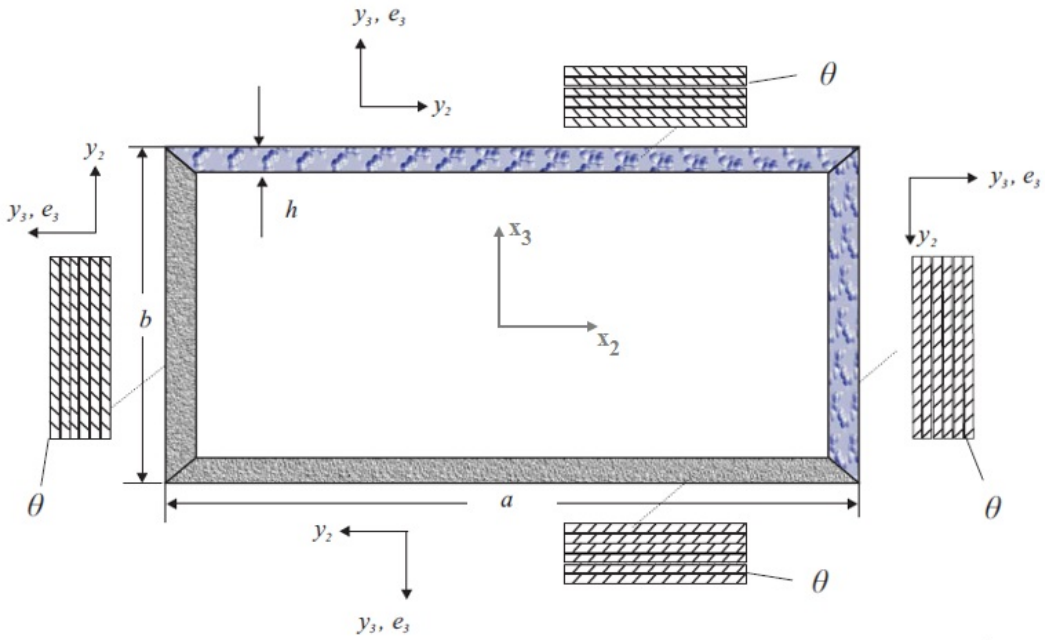

Figure 3.6: VABS layup convention for a box-beam[1].

3.3 Mass and Stiffness Matrices

From the finite element mesh of the cross-section with all geometric and material information specified, VABS calculates the cross-sectional properties.
In the VABS method[1], the local coordinate of a beam with an arbitrary cross-section is given in Figure - 3.2. The mass matrix with respect to the local beam coordinate system is given by[1]:

$$\begin{bmatrix} \mu & 0 & 0 & 0 & \mu x_{m3} & -\mu x_{m2} \\ 0 & \mu & 0 & -\mu x_{m3} & 0 & 0 \\ 0 & 0 & \mu & \mu x_{m2} & 0 & 0 \\ 0 & -\mu x_{m3} & \mu \mathrm{x_{m2}} & \mathrm{i_{22}}+\mathrm{i_{33}} & 0 & 0 \\ \mu x_{m3} & 0 & 0 & 0 & \mathrm{i_{22}} & \mathrm{i_{23}} \\ -\mu x_{m2} & 0 & 0 & 0 & \mathrm{i_{23}} & \mathrm{i_{33}} \end{bmatrix} \tag{3.1}$$

where μ is the mass per unit length, $(x_{\mathrm{m2}}, x_{\mathrm{m3}})$ is the mass center location, i_{23} is the product of inertia, i_{22} and i_{33} are the mass moment of inertia about x_2 and x_3 axes, respectively.
The classical 4×4 stiffness matrix is given by Equation-3.2[1].

$$\begin{Bmatrix} F_1 \\ M_1 \\ M_2 \\ M_3 \end{Bmatrix} = \begin{bmatrix} \bar{S}_{11} & \bar{S}_{12} & \bar{S}_{13} & \bar{S}_{14} \\ \bar{S}_{12} & \bar{S}_{22} & \bar{S}_{23} & \bar{S}_{24} \\ \bar{S}_{13} & \bar{S}_{23} & \bar{S}_{33} & \bar{S}_{34} \\ \bar{S}_{14} & \bar{S}_{24} & \bar{S}_{34} & \bar{S}_{44} \end{bmatrix} \begin{Bmatrix} \bar{\gamma}_{11} \\ \bar{\kappa}_1 \\ \bar{\kappa}_2 \\ \bar{\kappa}_3 \end{Bmatrix} \equiv \bar{S} \begin{Bmatrix} \bar{\gamma}_{11} \\ \bar{\kappa}_1 \\ \bar{\kappa}_2 \\ \bar{\kappa}_3 \end{Bmatrix} \tag{3.2}$$

where F_1 is the sectional axial force, M_1 is the sectional torque, M_2 and M_3 are the sectional bending moments around x_2, and x_3, respectively. Here, $\bar{S}$ is the stiffness matrix. $\bar{\gamma}_{11}$ is the beam axial stretching strain measure, $\bar{\kappa}_1$ is the twist measure, $\bar{\kappa}_2$ and $\bar{\kappa}_3$ are the curvature measures around the x_2 and x_3 axes, respectively[1].
Depending on the choice of the beam coordinate system, geometry, material and initial curvature/twist, the stiffness constants, $\bar{S}_{\mathrm{ij}}$ are formed. For example, for an isotropic prismatic beam with the x_2 and x_3 axes aligned with the principal bending axes and the beam reference line located in the tension center, the stiffness matrix is

by Equation-3.3[1].

$$\begin{bmatrix} EA & 0 & 0 & 0 \\ 0 & GJ & 0 & 0 \\ 0 & 0 & EI_2 & 0 \\ 0 & 0 & 0 & EI_3 \end{bmatrix} \tag{3.3}$$

If x_2 and x_3 axes of the isotropic prismatic beam are not aligned with the principal bending axes and the beam reference line is not located in the tension center, the stiffness matrix turns into the form given by Equation-3.4:

$$\begin{bmatrix} EA & 0 & S_3 & -S_2 \\ 0 & GJ & 0 & 0 \\ S_3 & 0 & EI_2 & -EI_23 \\ -S_2 & 0 & -EI_23 & EI_3 \end{bmatrix} \tag{3.4}$$

with $S_\alpha =< Ex_\alpha >$ and $EI_{23} =< Ex_2x_3 >$ where $< \cdot >= \iint \cdot \, dx_2 \, dx_3$.
The 6×6 stiffness matrix of the Timoshenko model is given by Equation-3.5[1]:

$$\begin{Bmatrix} F_1 \\ F_2 \\ F_3 \\ M_1 \\ M_2 \\ M_3 \end{Bmatrix} = \begin{bmatrix} S_{11} & S_{12} & S_{13} & S_{14} & S_{15} & S_{16} \\ S_{12} & S_{22} & S_{23} & S_{24} & S_{25} & S_{26} \\ S_{13} & S_{23} & S_{33} & S_{34} & S_{35} & S_{36} \\ S_{14} & S_{24} & S_{34} & S_{44} & S_{45} & S_{46} \\ S_{15} & S_{25} & S_{35} & S_{45} & S_{55} & S_{56} \\ S_{16} & S_{26} & S_{36} & S_{46} & S_{56} & S_{66} \end{bmatrix} \begin{Bmatrix} \gamma_{11} \\ 2\gamma_{12} \\ 2\gamma_{13} \\ \kappa_1 \\ \kappa_2 \\ \kappa_3 \end{Bmatrix} = S \begin{Bmatrix} \gamma_{11} \\ 2\gamma_{12} \\ 2\gamma_{13} \\ \kappa_1 \\ \kappa_2 \\ \kappa_3 \end{Bmatrix} \tag{3.5}$$

Here, $2\gamma_{12}$ and $2\gamma_{13}$ are the engineering transverse shear strains. The barred stiffness quantities in Equation-3.2 and unbarred stiffness quantities in Equation-3.5 are related as $\bar{(\,)} = (\,)|_{2\gamma_{12}=2\gamma_{13}=0}$.
In the stiffness matrix, S_{11} is the extensional stiffness, S_{22} and S_{33} are the shear stiffnesses, S_{44} is the torsional, and, S_{55} and S_{66} are the bending stiffnesses. Non-diagonal stiffness terms are the coupling stiffnesses. For example, S_{45} and S_{46} are the bending-torsion coupling stiffness quantities.

3.4 Theory of GEBT

The Geometrically Exact Beam Theory (GEBT) is developed by Prof. Hodges of Georgia Institute of Technology[15] and there is also an open source tool with the same name of the theory. In the book of Hodges[15], the beam theories are described deeply in Chapter 5. This chapter can be referred to for the formulation of the beam theories.

With respect to the selection of the variables, the formulation behind the beam analysis changes. For instance, DYMORE[16], which is a general purpose multibody dynamic code, is based on a displacement based formulation; in others word, the variables in the beam analyses are displacements/rotations. In this study, the 1D beam theory is based on a mixed variational formulation in which forces/moments, displacements/rotations, and momenta are used as variables. By using these variables, beams are analyzed statically and dynamically.

By using the cross-sectional characteristics obtained in VABS, GEBT gives the global behavior of the slender body. For each different cross-section in the beam, one cross-sectional analysis is performed by VABS. By using these results, for different load cases and boundary conditions, beam is analyzed by GEBT. If detailed three-dimensional information is required for the cross-section, the sectional loads obtained from the GEBT analyses are submitted to the VABS to recover the necessary 3D results, such as stresses and strains. In the output of GEBT, forces, moments and momenta are given in the deformed beam coordinate whereas displacements and rotations are in the undeformed global coordinate system. In GEBT, the right-hand coordinate system shown in Figure - 3.2 is used.

By specifying the geometric location of the nodes and the node connectivity information of the elements to GEBT, one-dimensional beam elements are easily created. Static, eigenvalue and transient beam analyses can be readily performed depending on the requirements of the outputs. The geometrically linear and nonlinear solutions of a problem is possible by GEBT as long as the problem is subjected to the small strain. Also, the number of iterations and the number of steps can be controlled depending on the problem. Depending on the analysis type, requirements of the inputs change[2]. For each node, the boundary conditions and loads must be defined in detail. For each cross-section, the structural properties must be given as input. If the analysis type is

not a static analysis, the inertial properties must be also set. For different analysis, the geometrically exact results for the beam are obtained.
There are many differences between the cross-sectional analysis and the finite element analysis methodologies. The order of the convergence is a difference between FEM and GEBT. In the study of Yu & Blair[17], it is indicated that; since GEBT uses a mixed variational formulation, the convergence of GEBT is different from the convergence of the finite element method. The convergence order of displacement-based finite element method is first displacements, then rotations, and then moments and forces . Whereas the convergence of GEBT analysis begins with the forces, then the moments, and the rotations, and ends with the displacements.

3.5 Advantage and Disadvantages of GEBT Analysis

There are many advantages of the GEBT. They are listed as follows:

- Geometrically Exact Beam Theory handles all geometric nonlinearities caused by large deflections and rotations, subject to the small strains. The capability to capture all geometric nonlinearities is very crucial for air vehicles since very flexible slender components are used to design them.

- By Geometrically Exact Beam Theory (GEBT), nonlinear analysis of a three-dimensional (3D) slender problem is reduced to a linear cross-sectional (2D) analysis and nonlinear beam (1D) analysis[2]. By this analysis methodology, the computing time of the 3D slender problem is reduced tremendously compared to the finite element method. This is the main advantage of the GEBT analyses over the finite element analyses.

- The formulation behind GEBT is the mixed variational in the weakest form. In other words, the lowest possible shape functions are utilized. By this selection, the integration can be calculated analytically by eliminating the numerical integration errors[17]. In another source[2], it is highlighted that, without any numerical integration and with the use of the lowest possible shape functions and the element matrices are determined exactly by GEBT.

- Moreover, by geometrically exact beam theory, the complete set of variables is directly determined due to the usage of the mixed variational formulation. To illustrate, for static analysis, displacements, rotations, forces and moments are found in all three dimensions.
- In GEBT, dynamic link libraries (DLLs) are used. DLLs are the file formats that are created for the purpose of using the information at the same time between many programs. Thus, it is very suitable to use the GEBT in other environments.

There are also some restrictions in using the cross-sectional analyses which are listed below:

- In GEBT, small strain assumption is made. Therefore, for large strain problems GEBT cannot be used.
- To be able to use GEBT, the geometry must be appropriate to be modeled as a beam.
- If the structure is not a slender body, beam analysis is not convenient.
- The cross-sectional analysis is very good to use in the preliminary design phase of the projects. However, for the critical regions, it is necessary to perform the detailed finite element analyses. For example, for the root of a helicopter blade, 3D effects are dominant and it is not possible to analyze it correctly without FEA.

CHAPTER 4

GENERATION OF THE BEAM-BLADE MODELS

Three different beam-blade models are used in this study. These models range from basic to complicated; composite rectangular cross-section, aluminum airfoil profile and composite airfoil profile. They are explained in detail in the subsections of this chapter.

An experimental helicopter tail rotor blade is used as the blade model in the present study. Blade model refers to this blade throughout the thesis. The used blade model is the preliminary configuration of the specified experimental helicopter model in Table - 4.1. The blade model is analyzed by excluding the root and the transient regions of the blade since in these regions 3D effects are dominant. It should also be noted that there is no geometric twist in the model.

Table 4.1: Tail Rotor Properties of the Experimental Helicopter.

Characteristics of Tail Rotor Blade	
Number of blades	2
Rotor Diameter [m]	1.8
Span [m]	0.9
Blade Cross-section	NACA 23012

4.1 Generation of the FEM Models

4.1.1 Finite Element Model Description of the Beam-Blade with the Composite Rectangular Cross-Section

As the first model, a rectangular cross-section beam with 6-meter span and no twist is chosen. In the FE model, surfaces of the beam are meshed with linear quadrilateral shell elements, (CQUAD4) in Patran and total of 5000 elements are used in the model. The whole model and the cut-out from a middle location of the model are shown in Figure - 4.1.

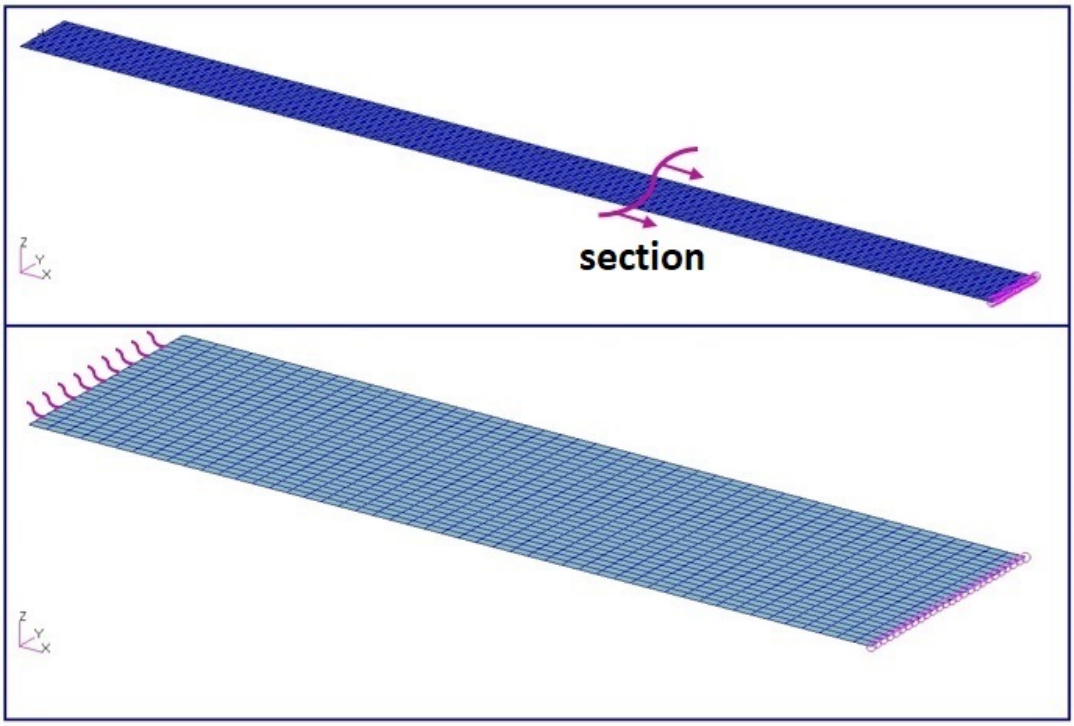

Figure 4.1: Finite element model of the rectangular cross-section.

In the rectangular cross-section beam, 8-plies exist in the thickness direction and the beam has a total thickness of 30 mm. Layered shell elements are used to model the composite laminate. The layup of the composite is set as $[0/90/45/-45]_{\mathrm{s}}$ which is balanced and symmetric. The cross-section of the rectangular model is presented in Figure - 4.2. Material properties of the ply material are presented in Table - 4.2[18].

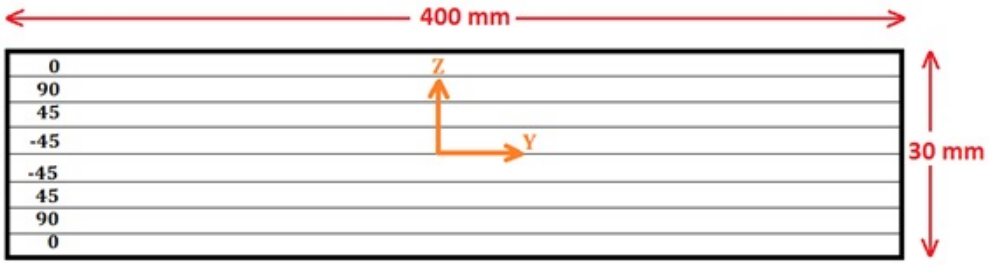

Figure 4.2: Rectangular cross-section.

Table 4.2: Material properties of the ply material in rectangular cross-section[18].

$E_1 = 132.38$ GPa, $E_2 = 10.76$ GPa, $\upsilon_{12} = 0.24$,
$G_{12} = G_{13} = 5.66$ GPa, $G_{23} = 3.38$ GPa

The boundary conditions and load applied are shown in Figure - 4.3. As for the boundary condition, six degrees of freedom of the nodes at the root are fixed. Loads are applied at the middle node at the tip of the beam. By using a rigid body element, RBE3, loads are distributed from this node to the all nodes at the tipoff the beam.
In the linear static user's guide of MSC. Nastran 2012[19] the details of rigid body elements are described. RBE2 is used for the rigid body connections whereas RBE3 is useful for distributing mass and load in the model. There is no additional stiffness coming to the structure due to the used of RBE3.

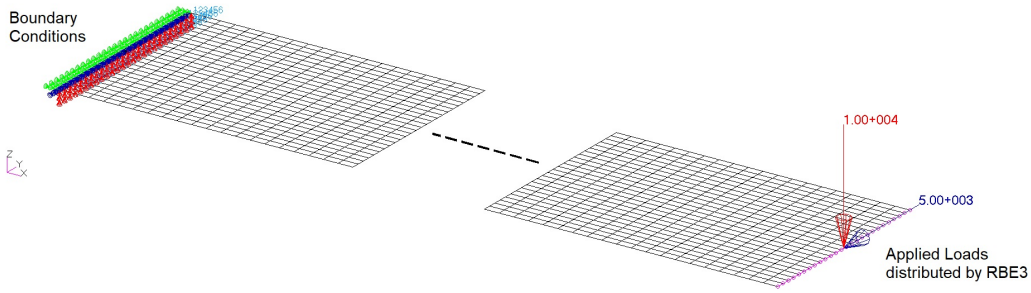

Figure 4.3: BCs and loads of the rectangular cross-section FEM model.

4.1.2 Finite Element Model Description of the Aluminum and Composite Blades with Airfoil Profile

As blade models, an isotropic aluminum and a composite model are selected. The chord of the blade is $180[mm]$ whereas the span is $900[mm]$ as given in Table - 4.1. The only difference between the aluminum and composite blade model is the material definition. The reason of the necessity of the aluminum blade model is the convenience it provides in modifying the model. For the aluminum blade model, instead of the composite laminate material, isotropic aluminum material properties are used for the entire shell elements. The element type of linear quadrilateral shell elements, CQUAD4, is used to mesh both the composite and isotropic blades.
Mesh size study is performed for the blade models. Three different mesh sizes are used. The tip displacement and Maximum Von Mises Stress results are plotted for three element sizes as shown in Figure - 4.4 and Figure - 4.5, respectively.

Figure 4.4: Mesh study of blade models (tip displacement variation).

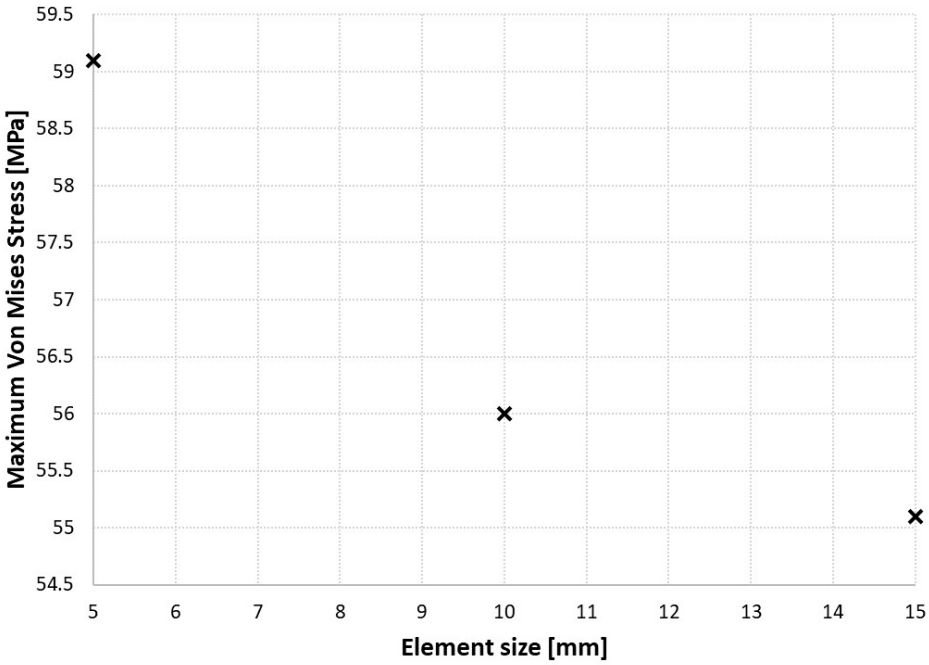

Figure 4.5: Mesh study of blade models (Maximum Von Mises Stress variation).

In the pursuing analyses, $5[mm]$ element size is chosen for the blade models in order not to increase analysis time. There are 3780 CQUAD4 elements in the blade models.

Composite laminate is modeled with layered shell elements so there is no normal stress component in the thickness direction in the finite element results. The layup of the composite blade is made up of S2/Glass fibers and epoxy resin. The ply orientations of the composite tail rotor blade are shown in Figure - 4.6. As it is seen from Figure - 4.6, different laminates are used in the spar and web region in the current configuration of the blade.

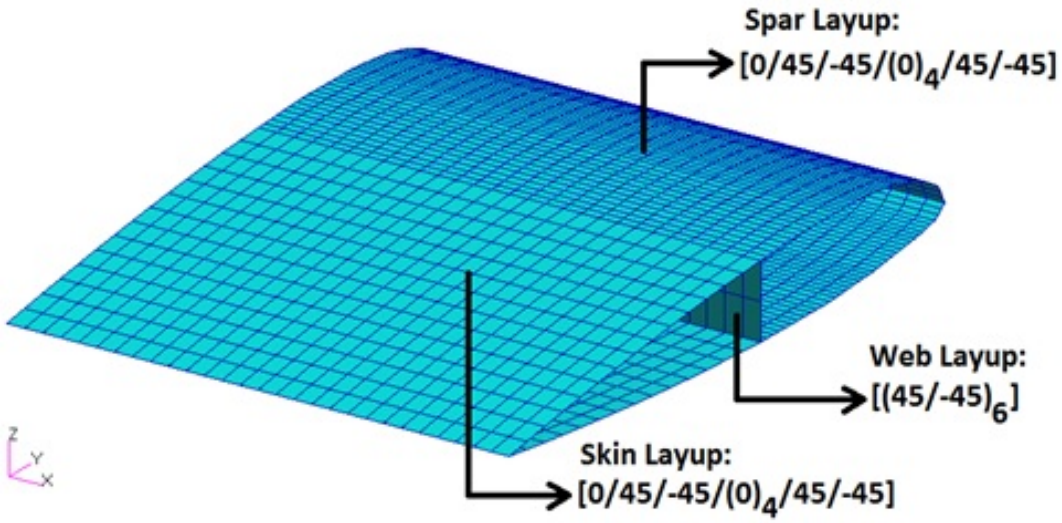

Figure 4.6: Layups of the FEM model of the composite blade.

Blade is fixed at the root and loaded at the tip at the neutral axis or at the shear center. If tension load is applied, neutral axis is selected as the load application point in order not to have bending at the end of the analysis. Moreover, if shear force is the load that the blade is subjected to, shear center is chosen since there will be no twist at the end of the analysis provided that the shear center location is calculated correctly.

At the beginning, there is no node in the FE model at the neutral axis or the shear center. Therefore, at first, two nodes, one at the root and other one at the tip, are created at the tension or at the shear center according to the applied load. Then, MPC-elements are introduced to connect these nodes to the root and tip cross-sections. As mentioned before, in MSC. Nastran, RBE2 type is suitable in the root region because it provides a rigid connection whereas RBE3 is more applicable at the tip since the purpose is to distribute load[19].

In Figure - 4.7, two parts of the blade are shown with root and tip elements. In the root part, the six-degree-of-freedoms are fixed at the node where RBE2 is connected to the nodes of the root cross-section. At the tip part, 250N flapwise bending force is applied at the node where RBE3 connected to the nodes of the tip cross-section. In Figure - 4.7, RBEs are shown in pink, and boundary conditions in blue color.

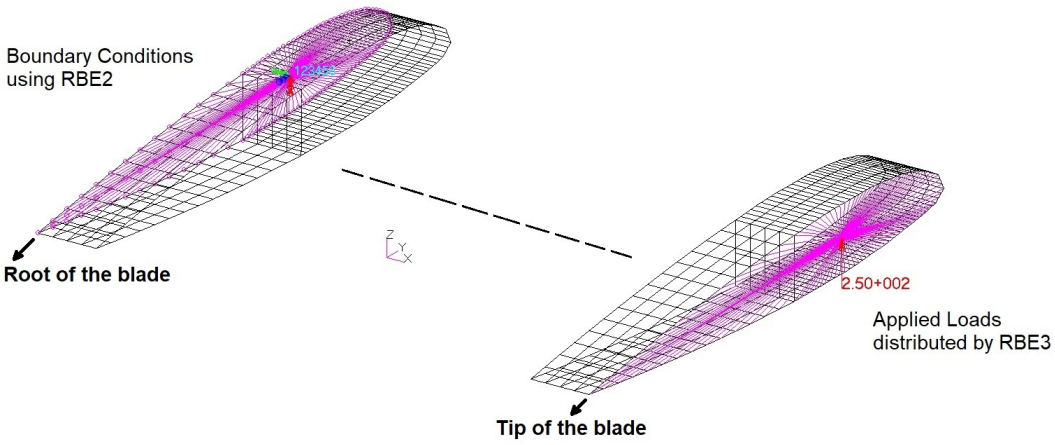

Figure 4.7: BCs and Loads of the blade FEM model.

4.2 Generation of the VABS and GEBT Models

The flowchart shown in the Figure - 3.1 is followed to generate the cross-section and the beam models. The details of the modeling is described in this section.

4.2.1 VABS and GEBT Model Descriptions of the Composite Rectangular Cross-Section

It is not possible to create a rectangular cross-section in PreVABS, because PreVABS is developed to generate airfoil type cross-sections. Therefore, for the cross-sectional analysis, the required shell elements in the cross-section are created in MSC. Patran. In MSC. Patran, a rectangle with the chord length of 400mm and total thickness of 30mm, shown in Figure - 4.2 is meshed using the linear quadrilateral shell elements, CQUAD4. In the cross-section 200 elements are used. The ply material property given in Table - 4.2 is set and the input file of MSC. Nastran is created. From the Nastran input file, coordinates of the nodes, element connectivity and material property information are taken. Layup and the ply plane angle for each element are added to generate the VABS input file. An example of a VABS input file is given in Figure - A.1.

As mentioned in the previous chapter, Timoshenko stiffness matrix is 6×6 ($S_{\text{ij}}, i, j = 1, 2, .., 6$). The diagonal terms are: S_{11} is the extensional stiffness, S_{22} and S_{33} are

the shear stiffnesses, S_{44} is the torsional, and, S_{55} and S_{66} are the bending stiffnesses. Non-diagonal stiffness terms are the coupling stiffness terms. As an example, S_{15} and S_{16} are the extension-bending coupling stiffness quantities[1].
By performing VABS analysis, the Timoshenko stiffness matrix of the rectangular cross-section model, shown in Figure - 4.2, is calculated as shown in Table - 4.3.

Table 4.3: Timoshenko Stiffness matrix of the rectangular cross-section.

6.210E+08 [N]	6.811E+05 [N]	3.191E-07 [N]	1.021E-04 [Nm]	-1.249E-04 [Nm]	-1.073E-04 [Nm]
6.811E+05 [N]	1.979E+08 [N]	-2.559E-06 [N]	-1.471E-04 [Nm]	1.116E-05 [Nm]	7.571E-05 [Nm]
3.191E-07 [N]	-2.559E-06 [N]	3.797E+07 [N]	6.045E-04 [Nm]	5.267E-05 [Nm]	9.944E-06 [Nm]
1.021E-04 [Nm]	-1.471E-04 [Nm]	6.045E-04 [Nm]	3.040E+10 [Nm^2]	-4.106E+09 [Nm^2]	-1.734E-02 [Nm^2]
-1.249E-04 [Nm]	1.116E-05 [Nm]	5.267E-05 [Nm]	-4.106E+09 [Nm^2]	7.597E+10 [Nm^2]	2.187E-02 [Nm^2]
-1.073E-04 [Nm]	7.571E-05 [Nm]	9.944E-06 [Nm]	-1.734E-02 [Nm^2]	2.187E-02 [Nm^2]	8.154E+12 [Nm^2]

After the stiffness matrix is obtained, the beam is modeled by GEBT. An example of a GEBT input file is given in Figure - A.2. The length of the beam is set as 6-meter and the calculated stiffness matrix of the rectangular cross-section in Table - 4.3 is assigned to the beam. The six degrees of freedom of the node at the root of the beam are set as zero to simulate the fixed end boundary condition. And, the load is applied from the node at the tip. In GEBT, two input files are created for two different load cases which are linear static and transient. The detailed information on the results of the GEBT analysis is given in Chapter 4.

4.2.2 Cross-Sectional and Beam Models of the Aluminum and Composite Blades

The cross-sectional analysis of the blade is performed by using PreVABS, VABS and GEBT. A meshed cross-section of the blade obtained by PreVABS is given in Figure

- 4.8. This example belongs to the model shifted to the shear center; in other words, the new origin of the blade cross-section is the shear center (the details of the shifting procedure are described in the next paragraphs). In the blade cross-section there are total of 1782 shell elements which are composed of the 4-noded quadratic elements that are the green elements and 3-noded triangular elements that are the blue ones in Figure - 4.8. It should be noted that at the trailing edge of the blade and the web connection parts, PreVABS generates triangular meshes. To compare stress results with FEM, quadrilateral elements that are not in the vicinity of these regions are selected for better comparison of the results.

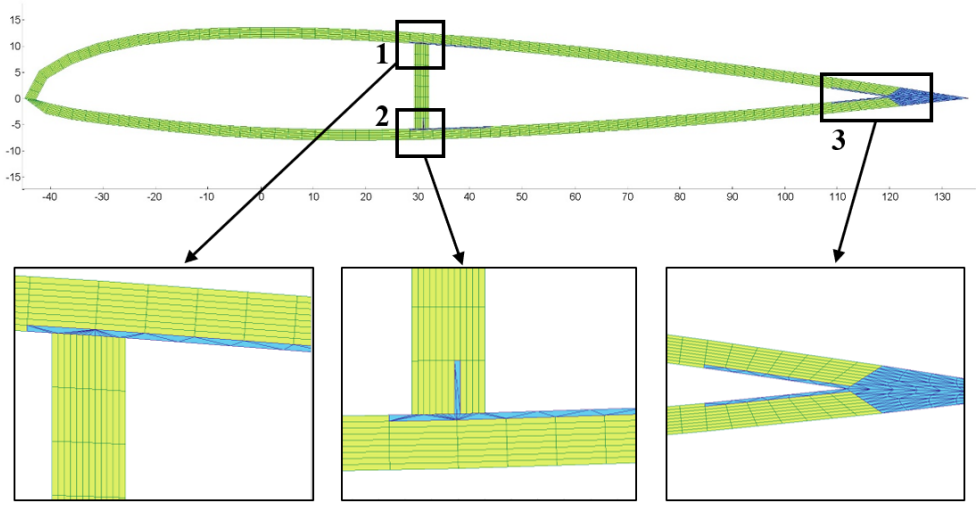

Figure 4.8: PreVABS mesh of the blade model.

In Figure - 4.9, the positive coordinate system definitions for the two analysis methods are shown. Throughout this thesis, positive Y (x_2) points from the trailing edge to the leading edge and positive X (x_1) points from root to the tip.

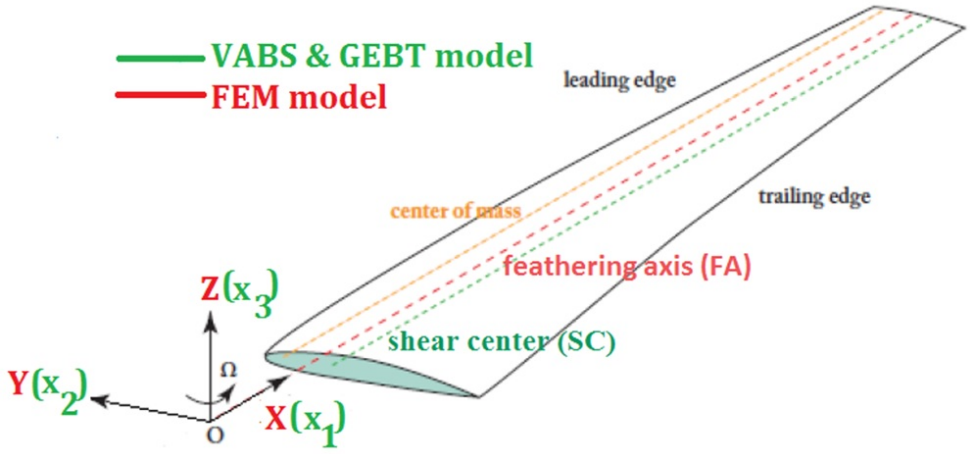

Figure 4.9: Positive coordinate system defined in VABS-GEBT and FE analysis.

In PreVABS, origin is aligned with the feathering axis (FA). The first VABS analysis is performed according to this origin and, in the output file, neutral axis (NA) and shear center (SC) locations are calculated with respect to the feathering axis. According to the type of the load applied in the particular analysis, the analyzed section is shifted so that the new origin becomes the tension or the shear center depending on the load type, such as tensile load or the shear load. For example, in Figure - 4.10, grey nodes show the cross-section with the origin at the feathering axis (FA) which is the default for the PreVABS analysis. If flapwise bending load is applied to this model, these grey nodes should be shifted as much as the calculated SC location so that the new VABS analysis should be done according to the new node locations shown with the black color in Figure - 4.10. When VABS analysis is performed with the black nodes as the FE nodes in PreVABS, calculated shear center location becomes the new origin at (0,0).

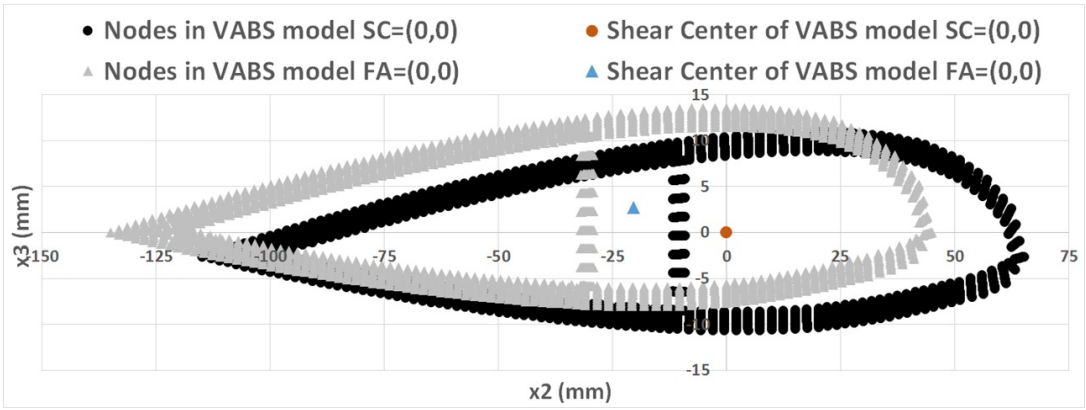

Figure 4.10: Node shifting strategy of the VABS analysis.

In the GEBT analysis, for the tension load case, force is applied through the tension center and Timoshenko stiffness matrix which is calculated with respect to the tension center is used in the analysis. For the shear load case, force is applied through the shear center and Timoshenko stiffness matrix calculated with respect to the shear center is used in the analysis.

In GEBT, the node at the root which is at the tension center or at the shear center depending on the applied load type in the analysis is fixed in six degrees of freedom and the load is applied from the node at the tip of the blade.

The Timoshenko stiffness matrix of the Aluminum blade model with the origin at the shear center is given in Table - 4.4. Also, the Timoshenko stiffness matrix of the composite blade with the origin at the shear center is given in Table - 4.5.

Table 4.4: Timoshenko stiffness matrix of the Aluminum blade with the origin at the shear center.

6.255E+07 [N]	0.000E+00 [N]	0.000E+00 [N]	0.000E+00 [Nm]	-3.456E+07 [Nm]	9.288E+08 [Nm]
0.000E+00 [N]	1.013E+07 [N]	1.291E+05 [N]	-1.337E-02 [Nm]	0.000E+00 [Nm]	0.000E+00 [Nm]
0.000E+00 [N]	1.291E+05 [N]	6.082E+05 [N]	-2.199E-03 [Nm]	0.000E+00 [Nm]	0.000E+00 [Nm]
0.000E+00 [Nm]	-1.337E-02 [Nm]	-2.199E-03 [Nm]	2.897E+09 [Nm^2]	0.000E+00 [Nm^2]	0.000E+00 [Nm^2]
-3.456E+07 [Nm]	0.000E+00 [Nm]	0.000E+00 [Nm]	0.000E+00 [Nm^2]	3.497E+09 [Nm^2]	-2.028E+09 [Nm^2]
9.288E+08 [Nm]	0.000E+00 [Nm]	0.000E+00 [Nm]	0.000E+00 [Nm^2]	-2.028E+09 [Nm^2]	1.047E+11 [Nm^2]

Table 4.5: Timoshenko stiffness matrix of the composite blade with the origin at the shear center.

2.368E+07 [N]	3.180E+01 [N]	9.859E+01 [N]	3.295E+05 [Nm]	-1.888E+07 [Nm]	4.879E+08 [Nm]
3.180E+01 [N]	5.076E+06 [N]	7.392E+04 [N]	2.863E+00 [Nm]	-1.906E+05 [Nm]	-4.871E+03 [Nm]
9.859E+01 [N]	7.392E+04 [N]	4.054E+05 [N]	1.549E+00 [Nm]	-3.052E+03 [Nm]	-1.385E+04 [Nm]
3.295E+05 [Nm]	2.863E+00 [Nm]	1.549E+00 [Nm]	1.067E+09 [Nm^2]	-2.692E+05 [Nm^2]	6.298E+06 [Nm^2]
-1.888E+07 [Nm]	-1.906E+05 [Nm]	-3.052E+03 [Nm]	-2.692E+05 [Nm^2]	1.228E+09 [Nm^2]	-1.363E+09 [Nm^2]
4.879E+08 [Nm]	-4.871E+03 [Nm]	-1.385E+04 [Nm]	6.298E+06 [Nm^2]	-1.363E+09 [Nm^2]	6.775E+10 [Nm^2]

In GEBT analyses, the calculated stiffness matrices for Aluminum and composite blades that are presented in Table - 4.4 and Table - 4.5, respectively, are assigned to the beams. Different GEBT input files are created for different load cases. The detailed information on the results of the GEBT analysis is given in Chapter 4.

CHAPTER 5

RESULTS OF THE BLADE MODELS

In the previous chapter, the details of the beam and 3D FE models are described. In this chapter, the results obtained by the geometrically exact beam and 3D finite element models are presented. Results are presented for the linear static, modal and transient analyses and linear and nonlinear analysis results obtained by the beam and the FE models.

As mentioned before; throughout the analyses, blade is fixed in six degree-of-freedom at the root in both 3D FE and geometrically exact beam analysis. Moreover, for the comparison of the stresses, elements at the mid-span are selected since they are not in the vicinity of any boundary condition.

In order to perform finite element analysis, MSC. Patran[20] is used as pre and post processor and MSC. Nastran[20] is used as the solver. For the beam analysis, VABS is used for the cross-sectional analysis and stress recovery, GEBT is used to perform the beam analysis.

5.1 Results of the Rectangular Cross-Section Model

5.1.1 Linear Static Analysis Results of the Rectangular Cross-Section Blade Model

For a simple rectangular cross-section composite blade, the element stresses are obtained with both VABS and finite element method for verification purposes.

In the rectangular cross-section model, $5000[N]$ chordwise and $10000[N]$ flapwise bending forces are applied together as shown in Figure - 4.3.

For the selected cross-section, VABS input file is created using the mesh information

from MSC. Patran due to the simplicity of the geometry. After the stiffness matrix is determined, the internal loads (sectional forces and moments) acting in this chosen section are calculated by GEBT. Applying the cross-sectional loads found from GEBT, VABS is rerun to recover the 3D strains and stresses. The differences of the stresses between FE analysis results and VABS analyses for various material orientations are presented in Table - 5.1. Since normal stresses in the thickness direction are zero, they are not shown in Table - 5.1.

Table 5.1: Differences of stresses [MPa] for rectangular cross-section between FEM & VABS under bending loading.

		$\sigma_{11}[MPa]$	$\tau_{12}[MPa]$	$\tau_{31}[MPa]$	$\sigma_{22}[MPa]$	$\tau_{23}[MPa]$
0-degree ply	FEM	687.70	-8.26	0.00	7.49	0.00
	VABS	684.16	-7.99	-0.45	7.60	0.19
90-degree ply	FEM	-42.70	5.95	-0.83	38.99	0.00
	VABS	-41.54	5.74	0.03	39.06	0.86
45-degree ply	FEM	92.62	-13.90	-0.88	15.94	0.00
	VABS	94.04	-13.85	-0.86	15.89	0.56
-45-degree ply	FEM	60.18	4.63	-0.99	3.47	0.00
	VABS	59.00	4.62	-0.56	3.54	-1.01

From Table - 5.1, it is seen that the stresses, especially the dominant ones, match perfectly for the two analyses. Therefore, it can be said that finite element method and cross-sectional analyses results are in good agreement in terms of in-plane stresses for shell elements under bending loading for the rectangular cross-sectional model with composite material.

5.1.2 Linear Transient Analysis of the Rectangular Cross-Section Model

The transient response of the rectangular cross-section model under time varying shear load shown in Figure - 5.1 is determined. The load application point is shown in Figure - 4.3. For the rectangular composite cross-section, the flapwise tip displacement results of the FE and GEBT model are shown in Figure - 5.2.

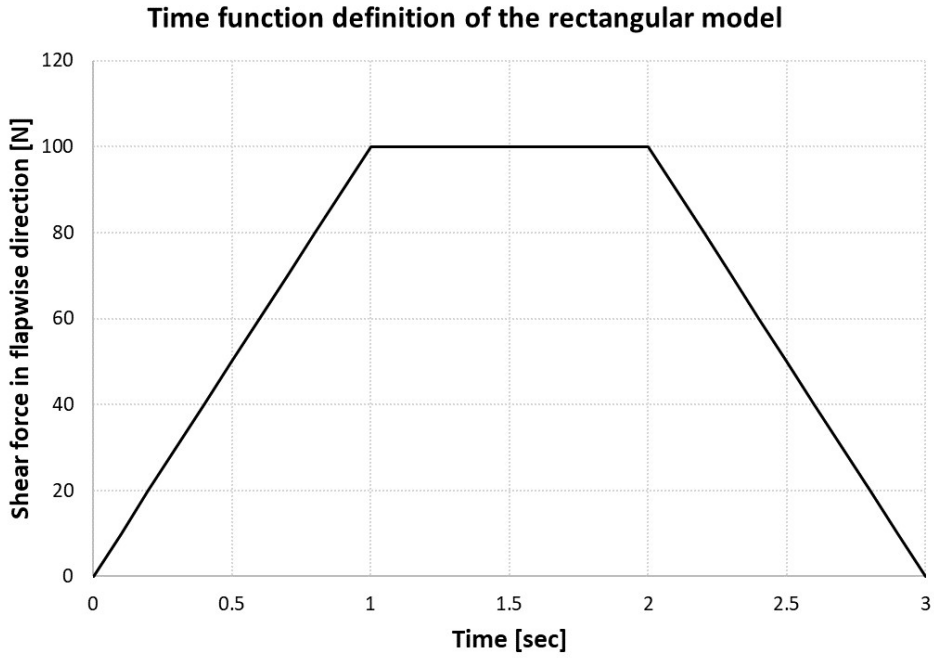

Figure 5.1: Time function definition of the rectangular cross-section model.

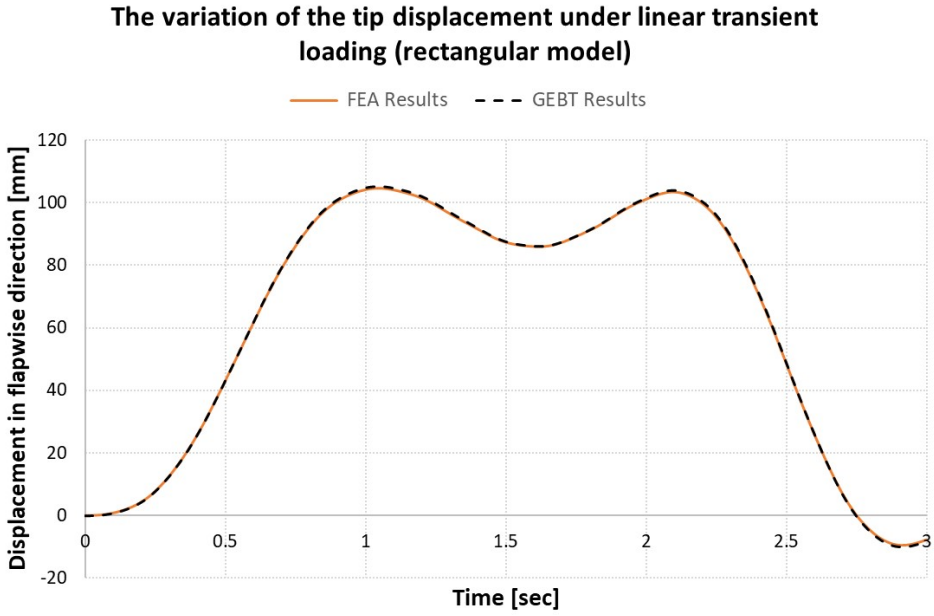

Figure 5.2: FE and GEBT transient analysis result of the rectangular cross-section blade model.

From the comparison given in Figure - 5.2, it can be said that transient responses of the two analysis methods match perfectly for a rectangular composite cross-section model.

However, the tip displacement response of GEBT and FE analyses are not as straight as the time function definition presented in Figure - 5.1. The cause of the waviness in Figure - 5.2 is investigated; and it is seen that the main reason is the length of the blade span. Since rectangular cross-section beam has a span of 6-meter, longer span beam has smaller stiffness and causes oscillations in the response. In addition, in the analysis model, since there is no damping oscillations continue throughout the transient analysis duration. The effect of the span length on the response of the beam is shown in Figure - 5.3. As seen in Figure - 5.3, shorter span beam also has oscillatory response but the magnitude of the oscillations is very small.

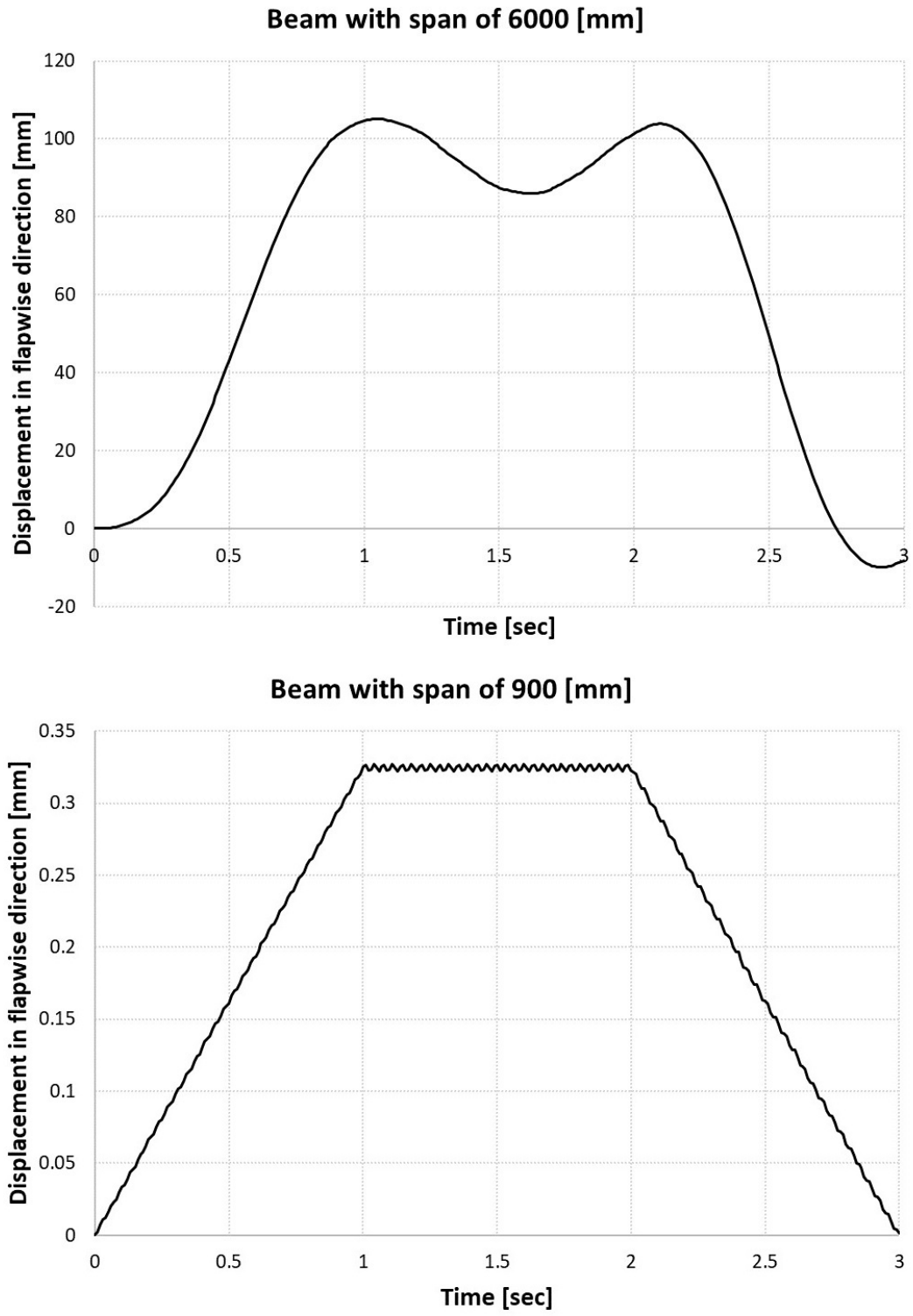

Figure 5.3: Effect of the span of the beam in the transient analysis of the rectangular cross-section blade model.

5.2 Results of the Aluminum Blade

5.2.1 Modal Analysis of the Aluminum Blade

In order to see the cross-section complexity effect on the comparison study without material complexity, an Aluminum airfoil profile is chosen which is shown in Figure - 4.8. The blade with Aluminum airfoil profile is analyzed to get the natural frequencies of the blade by FE and GEBT methods. The comparison of the first five eigenvalues is presented in Table - 5.2. The first four modes are 1st flapwise bending, lead-lag, 2nd flapwise bending and torsion, respectively.

Table 5.2: Comparison of the results of the modal analysis for the Aluminum blade.

Eigenvalue No - Mode Shape	Eigenvalue results of GEBT [Hz]	Eigenvalue results of FEM [Hz]
1- 1st flapwise bending	25.67	25.12
2- lead-lag	130.22	132.52
3- 2nd flapwise bending	146.72	144.87
4- torsion	248.35	232.33
5- 3rd flapwise bending	365.93	361.18

From Table - 5.2, it is seen that the natural frequencies of the Aluminum blade determined by the FE analysis and GEBT agree very well. The difference of the natural frequencies is less than 2% except for the torsion mode.

5.2.2 Transient Analysis of the Aluminum Blade

The transient analysis of the Aluminum blade is performed by both FEM and GEBT. To simulate the transient response of the Aluminum blade, the time varying load is applied at the shear center location at the blade tip, as shown in Figure - 4.7. Time varying load is presented in Figure - 5.4. This flapwise shear load is introduced in the FE and GEBT models, and their tip displacement results are given in Figure - 5.5.

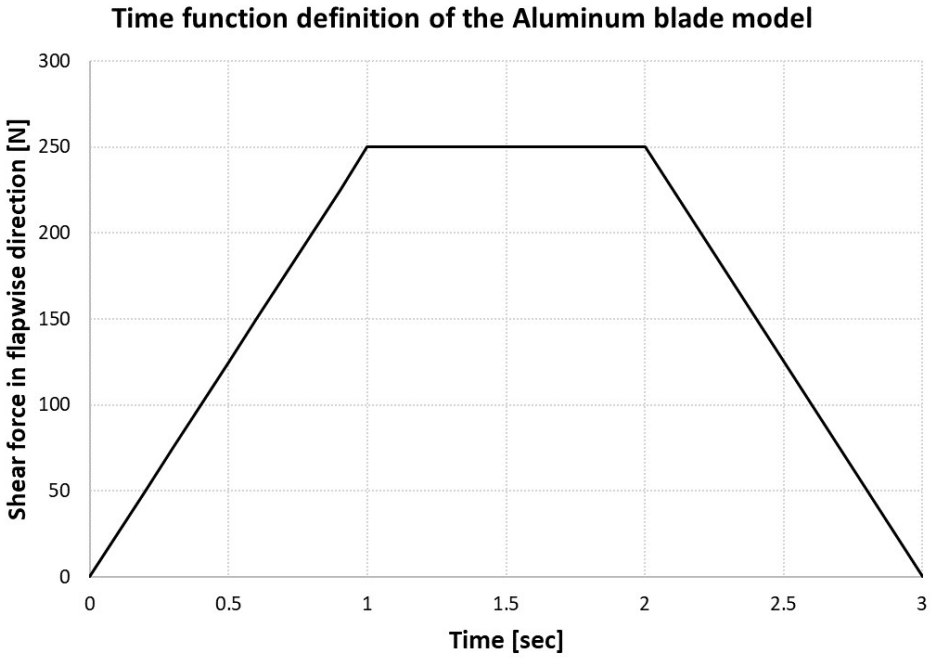

Figure 5.4: Time function definition of the Aluminum blade.

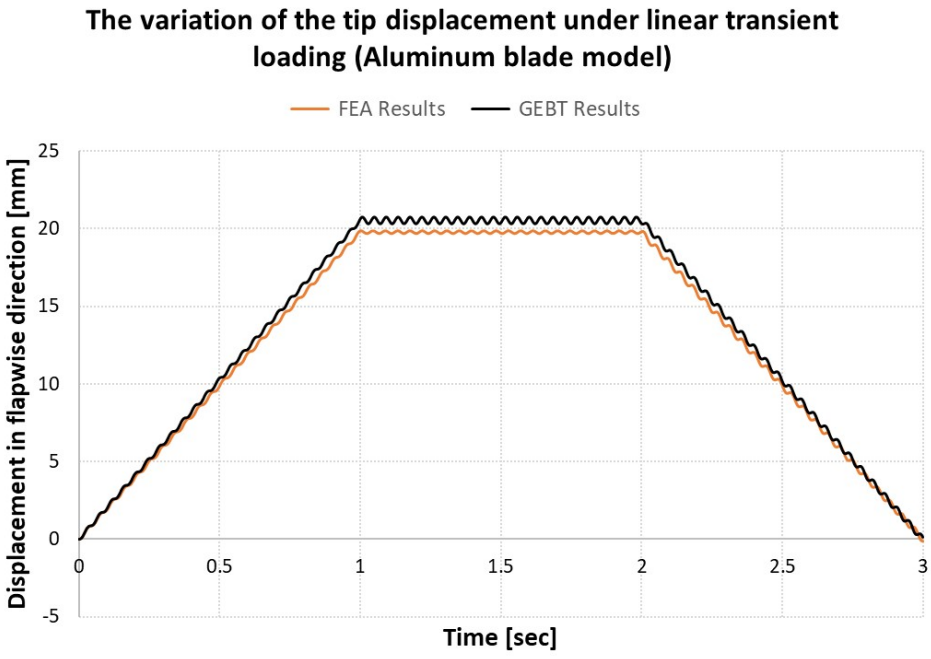

Figure 5.5: Variation of the tip displacement in flapwise direction of the Aluminum blade obtained by FE and GEBT analysis.

From Figure - 5.5, it is seen that there is a small difference in the displacements between two analysis methods. Thus, the transient responses of the Aluminum blade model obtained by the finite element analysis and GEBT analysis are in good agreement.

5.3 Results of the Composite Blade

In this section, the results of the composite blade are presented. The boundary conditions and the loads of the finite element model are shown in Figure - 4.7 and composite layup is given in Figure - 4.6. Also, the mesh of the cross-section model obtained by PreVABS is shown in Figure - 4.8.
In MSC. Nastran, for the layered shell elements, mid-ply stress values are given as output. In order to compare the stresses at the same location for the two analyses, stresses at the Gauss integration points are averaged in VABS analysis.
Figure - 5.6 shows the selected Gauss points where stresses are calculated by VABS. At the upper part of Figure - 5.6, the nodes of the whole elements in the VABS model are given in blue and the orange points are the Gauss integration points of the chosen elements for the comparison study. At the lower part of Figure - 5.6, a closer view of the chosen elements and their ply orientations are presented. As it is seen from Figure - 5.6, the selected elements are quadrilateral elements in the upper skin.

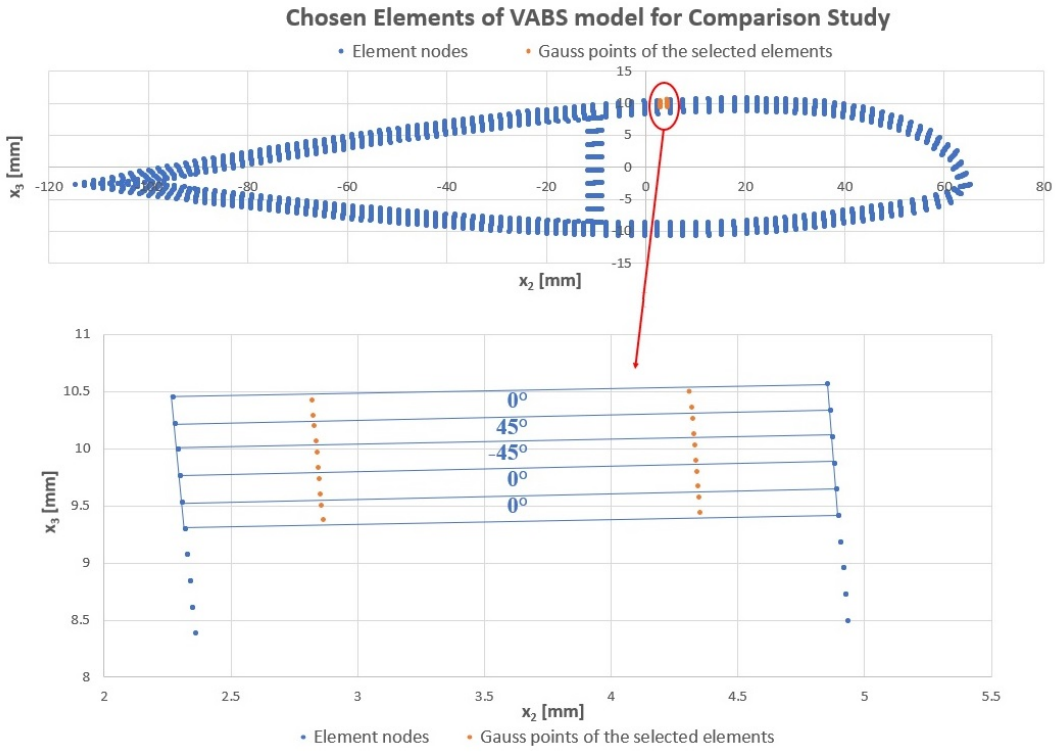

Figure 5.6: Selected Gauss points for the stress comparison study in VABS analysis.

As mentioned before; for the comparison study of the stress analysis, an element at the mid-span should be selected since it is not in the vicinity of any boundary condition. For this purpose, the element of the spar at STA442.5 is chosen. The selected station and the element is given in Figure - 5.7.

All the stress comparison studies of the composite blade are performed for the element shown in Figure - 5.7.

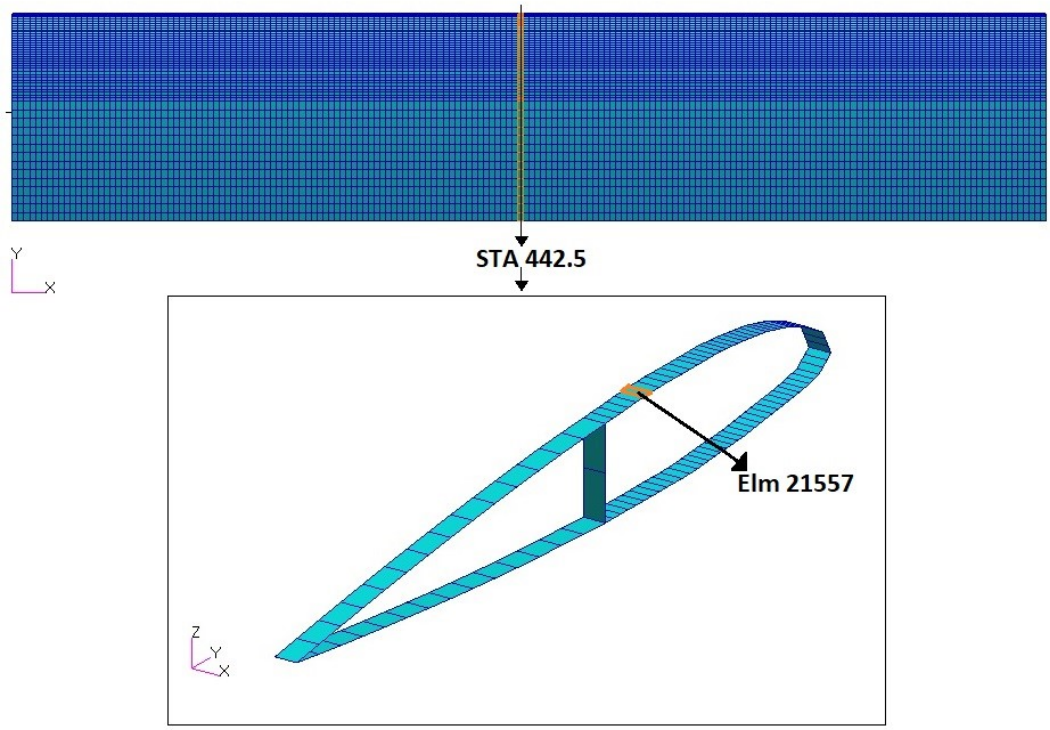

Figure 5.7: The element of the composite blade selected for the comparison study.

5.3.1 Modal Analysis of the Composite Blade

After the cross-sectional complexity effect on the comparison study is shown, the material complexity is added on the model by creating a model made of the composite material. To get the natural frequency response of the tail rotor blade, eigenvalue analyses are performed utilizing the finite element and the GEBT models of the blade. First four modes are ordered as: 1st flapwise bending, 2nd flapwise bending, lead-lag, and torsion mode. The natural frequencies of the blade are given in Table - 5.3.

Table 5.3: Comparison of the modal analysis results by the FE and GEBT analysis of the composite blade.

Eigenvalue No - Mode Shape	Eigenvalue results of GEBT [Hz]	Eigenvalue results of FEM [Hz]
1- 1st flapwise bending	19.92	19.32
3- 2nd flapwise bending	117.57	113.13
3- lead-lag	134.55	140.25
4- torsion	157.26	144.97
5- 3rd flapwise bending	305.02	288.71

Table - 5.3 shows that that the natural frequency results of the FE and GEBT models are in good agreement. Maximum of 7.8% difference exists between the eigenvalue analysis results of the two methods for the composite blade model.

5.3.2 Composite Blade under Tension Load (Linear Static Analysis)

For the composite blade model, linear static analysis response of the FEM and GEBT model is sought under the tension load. To obtain this result, models are transformed such that the neutral axis of the new model is taken as the origin and an axial force of $100 \times 10^3[N]$ is applied at the neutral axis.

The stress results in the spar layup of the model shown in Figure - 4.6 are compared. From outer to inner layer, at the station 442.5, stress results calculated by FE analysis and recovered by VABS are presented in Table - 5.4 for different plies of the element shown in Figure - 5.7. Since normal stresses in the thickness direction are zero, they are not shown in Table - 5.4.

Table 5.4: Comparison of stresses calculated by FE analysis and recovered by VABS under pure tension load case (linear analysis).

		$\sigma_{11}[MPa]$	$\tau_{12}[MPa]$	$\tau_{31}[MPa]$	$\sigma_{22}[MPa]$	$\tau_{23}[MPa]$
0-degree ply	FEM	179.27	0.08	0.00	-8.17	0.00
	VABS	187.57	0.09	0.01	-8.81	0.00
45-degree ply	FEM	57.72	-27.76	0.00	19.96	0.01
	VABS	59.26	-29.12	0.01	20.94	0.01
-45-degree ply	FEM	56.89	27.80	0.00	20.09	0.01
	VABS	60.03	29.12	0.01	20.75	0.01
0-degree ply	FEM	179.41	0.09	0.00	-8.40	0.01
	VABS	187.56	0.09	0.01	-8.85	0.01
0-degree ply	FEM	179.45	0.09	0.00	-8.48	0.01
	VABS	187.56	0.08	0.01	-8.86	0.01

It is seen from Table - 5.4 that, for the composite blade model under the tension load effect, the difference between the results of FE analysis and VABS for the dominant axial stresses is less than 5%. Thus, it can be highlighted that the composite blade model results under the tension load agree very well for two different analysis techniques.

5.3.3 Composite Blade under Shear Load (Linear Static Analysis)

As mentioned previously, at the end of the VABS analysis the shear center location of the section of the blade can be determined. The shear center location of the composite blade model calculated by VABS analysis is presented in Figure - 5.8.

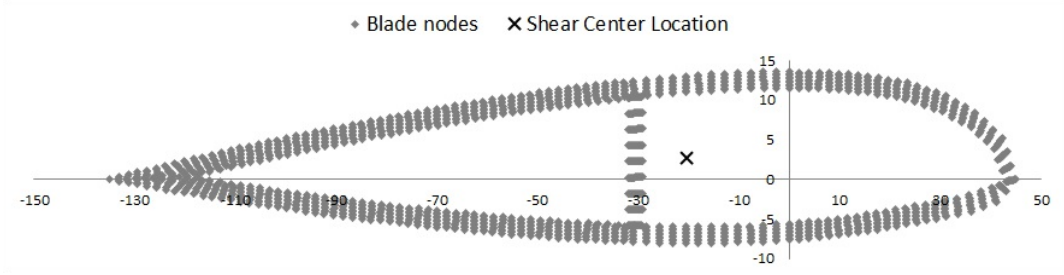

Figure 5.8: Shear Center location of the composite blade model.

In the FE model, the load is applied at this calculated shear center point. Whether the shear center location of the two analyses match or not is determined from the vertical displacement difference of the leading and trailing edge point of the tip section of the blade. If the difference between the leading and the trailing edge of the wing tip deflection is close to zero, it means that the twist of the wing is nearly zero and it can be concluded that the shear center location of the FE model is just about right. As shown in Figure - 5.9, for the $250[N]$ flapwise shear load application at the wing tip (which is shown in Figure - 4.7), there is 0.2% difference between the leading and the trailing edge vertical deflections at the wing tip. Therefore, it is considered that the shear center location of the FE model is at more or less correct location.

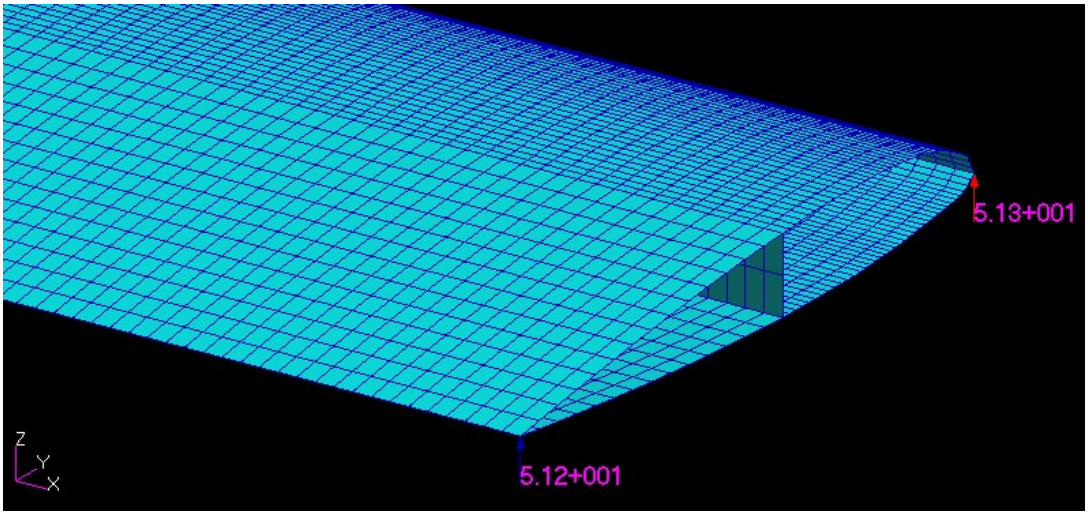

Figure 5.9: Verification of the shear center location in the FE model.

Comparison of the displacement in all three dimensions of the load application point at the tip is presented for FEM and GEBT model in Table - 5.5 for the $250[N]$ flapwise shear load.

Table 5.5: Displacement comparison of the load application point at the tip for the linear analysis under shear load.

	$u_1[mm]$	$u_2[mm]$	$u_3[mm]$
GEBT	-0.04	-0.87	51.31
FEM	-0.05	-0.82	51.28

It is seen from Table - 5.5 that displacement components of the load application point are in good agreement between two methods.
When the $250[N]$ shear load is applied at the shear center, the stresses determined in VABS and the finite element analysis, at the station 442.5 of the element shown in Figure - 5.7, are given in Table - 5.6. In Table - 5.6, stress results are given for plies from outer to the inner layer of the spar layup shown in Figure - 4.6. As before, because normal stresses in the thickness direction are zero, they are not presented in Table - 5.6.

Table 5.6: Differences of stresses [MPa] between FEM & VABS under shear load of the composite blade at STA442.5 (linear analysis).

		$\sigma_{11}[MPa]$	$\tau_{12}[MPa]$	$\tau_{31}[MPa]$	$\sigma_{22}[MPa]$	$\tau_{23}[MPa]$
0-degree ply	FEM	-38.64	0.50	0.00	1.92	0.00
	VABS	-45.77	0.42	0.00	2.13	0.00
45-degree ply	FEM	-10.26	6.19	0.00	-4.86	0.00
	VABS	-16.17	6.94	0.00	-4.56	0.01
-45-degree ply	FEM	-15.00	-6.33	0.00	-3.96	0.00
	VABS	-12.09	-6.79	0.00	-5.33	0.01
0-degree ply	FEM	-41.60	0.50	0.00	2.00	0.00
	VABS	-42.84	0.44	0.00	1.98	0.00
0-degree ply	FEM	-42.58	0.50	0.00	2.03	0.00
	VABS	-41.86	0.44	0.00	1.94	0.00

From Table - 5.6, it is seen that the stress resultants of the composite blade are in considerably good agreement with each other for the VABS and FE linear analysis under the shear load.

The solution time of the two analyses are given in Table - 5.7 for the linear static analysis of the composite blade model. The analysis time given for GEBT&VABS includes not only the stress recovery and but also the beam analysis. Table - 5.7 shows that analysis performed by the cross-sectional analysis (VABS & GEBT) lasts in a very short time compared to the FE analysis. This result shows that in repeated analysis involving optimization or time marching aeroelastic analysis, GEBT would have substantial advantages over the FE analysis in terms of computational time.

Table 5.7: Analysis time comparison of FEM and GEBT & VABS (linear static analysis of the composite blade).

Analysis Type	Time [sec]
FEM	31.42
GEBT & VABS	5.94

For the composite blade under $250[N]$ flapwise shear loading, the spanwise variation of the stresses is investigated. The fourth layer from the top (0°-ply) shown in Figure - 5.6 is selected for comparison of the spanwise stress variation. The axial stresses determined by VABS and the finite element analysis at different stations are plotted in Figure - 5.10.

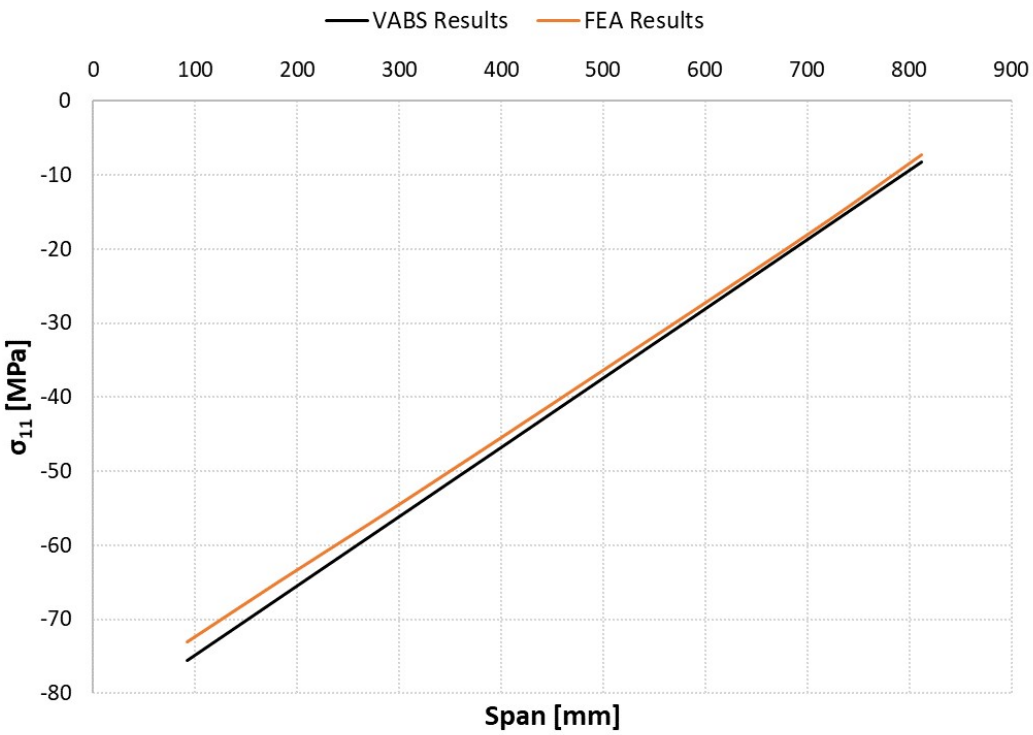

Figure 5.10: Change of the axial stresses along span of the composite blade model under shear loading (linear static analysis - $0°$ ply).

As seen from Figure - 5.10, the dominant axial stresses of the $0°$-ply are in good agreement for the finite element and VABS recovery analysis.

5.3.4 Composite Blade under Distributed Load (Linear Static Analysis)

The responses of the linear static analyses of both FE and GEBT are investigated under the distributed load. To obtain this result, models are transformed such that the web of the new model is taken as the origin and the flapwise shear force of $1250[N]$ is distributed from the web along span as shown in Figure - 5.11 and Figure - 5.12.

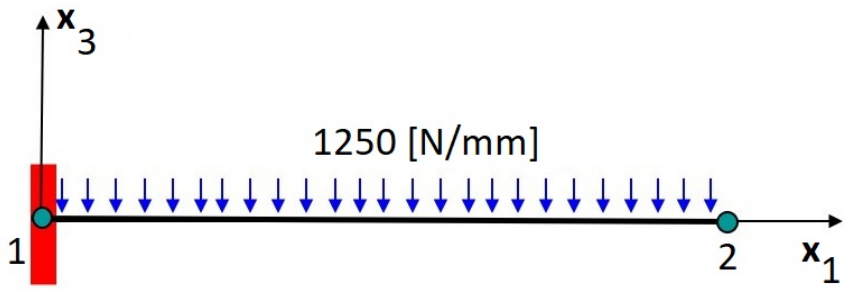

Figure 5.11: Distributed load definition of the beam model.

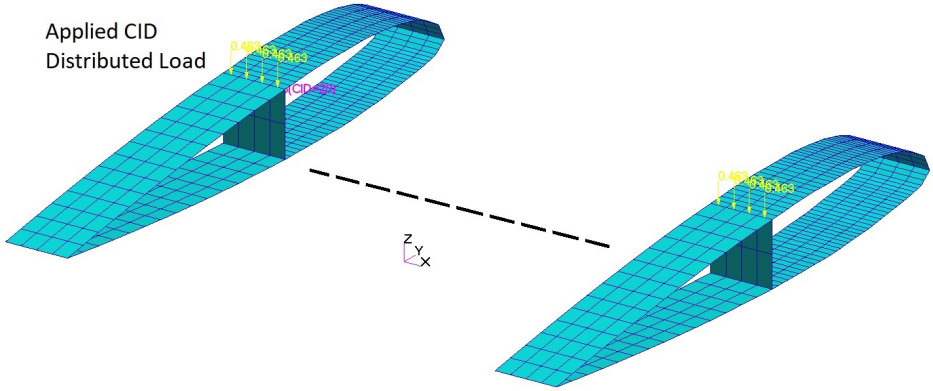

Figure 5.12: Distributed load definition of the FE model.

The stress results in the spar layup of the model shown in Figure - 4.6 are compared. From outer to inner layer, at the station 442.5, stress results calculated by FE analysis and recovered by VABS are presented in Table - 5.8 for different plies of the element shown in Figure - 5.7. Since normal stresses in the thickness direction are zero, they are not shown in Table - 5.8.

Table 5.8: Differences of stresses [MPa] between FEM & VABS under distributed load of the composite blade at STA442.5 (linear analysis)

		$\sigma_{11}[MPa]$	$\tau_{12}[MPa]$	$\tau_{31}[MPa]$	$\sigma_{22}[MPa]$	$\tau_{23}[MPa]$
0-degree ply	FEM	50.05	1.76	0.01	-0.35	0.04
	VABS	58.13	1.60	0.01	-0.52	0.00
45-degree ply	FEM	10.90	-7.38	0.01	8.34	0.10
	VABS	10.68	-8.85	0.00	7.81	-0.02
-45-degree ply	FEM	25.88	7.78	0.01	4.47	0.13
	VABS	25.05	8.65	-0.01	4.68	-0.03
0-degree ply	FEM	53.24	1.81	0.02	-2.27	0.14
	VABS	54.43	1.59	-0.03	-2.55	0.01
0-degree ply	FEM	54.30	1.82	0.02	-2.90	0.15
	VABS	53.20	1.59	0.00	-2.47	0.01

From Table - 5.8, it is seen that VABS and GEBT combination gives considerably well stress results for the distributed linear load case when compared with the solution of the finite element analysis.

5.3.5 Composite Blade under Shear Load (Nonlinear Static Analysis)

Next, the geometric nonlinearity effect is investigated for the composite blade model under the shear load. By performing GEBT static analysis linearly and nonlinearly, the load level that is appropriate for nonlinear analysis is determined. Under the $500[N]$ flapwise shear load, the variation of the axial displacement in the spanwise direction of the beam model is given in Figure - 5.13.

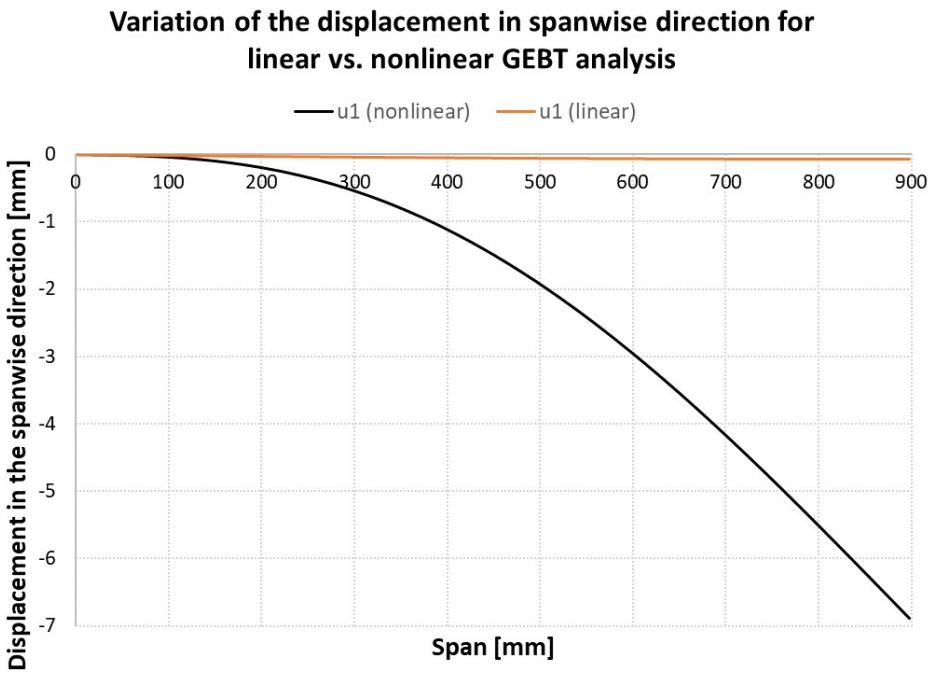

Figure 5.13: Variation of the axial displacement in the spanwise direction under shear load for linear and nonlinear GEBT static analysis.

Observing Figure - 5.13, it is obvious that $500[N]$ flapwise shear load is high enough to cause geometrically nonlinear deflection of the blade model. Therefore, the analyses are performed under this load case utilizing the nonlinear solution sequence SOL400 of Nastran for finite element analysis and nonlinear analysis option of GEBT. The displacement of the load application point determined by the geometrically nonlinear GEBT and the FE analyses are given in Table - 5.9. The positive direction of the displacements u_1, u_2, and u_3 can be seen from Figure - 4.9.

Table 5.9: Displacement comparison of the load application point at the tip for nonlinear analysis under shear load.

	u_1 – axial displacement [mm]	u_2 – edgewise displacement [mm]	u_3 – flapwise displacement [mm]
GEBT	-6.92	-1.71	101.27
FEM	-7.02	-1.88	101.86

It is noted that the displacement of the load application point for the geometrically

nonlinear GEBT and FE analyses are very close to each other for the shear load case. For the nonlinear static analyses of the composite blade, when the $500[N]$ shear load is applied at the shear center, the stresses determined by VABS and the finite element analysis at STA442.5 for the element shown in Figure - 5.7 are given in Table - 5.10. In Table - 5.10, as mentioned before, stress results are given for the plies from outer to the inner layer of the spar layup shown in Figure - 4.6. Also, because normal stresses in the thickness direction are zero, they are not presented in Table - 5.10.

Table 5.10: Differences of stresses between FEM & VABS under shear load of the composite blade at STA442.5 (nonlinear analysis).

		$\sigma_{11}[MPa]$	$\tau_{12}[MPa]$	$\tau_{31}[MPa]$	$\sigma_{22}[MPa]$	$\tau_{23}[MPa]$
0-degree ply	FEM	-75.77	-0.95	-0.02	4.13	0.11
	VABS	-90.28	-0.85	-0.01	4.19	0.00
45-degree ply	FEM	-20.10	12.23	-0.02	-9.29	0.25
	VABS	-23.97	13.69	0.00	-8.98	0.02
-45-degree ply	FEM	-28.55	-12.48	-0.03	-9.84	0.34
	VABS	-23.79	-13.39	0.01	-10.52	0.02
0-degree ply	FEM	-81.67	-0.78	-0.03	3.97	0.38
	VABS	-84.50	-0.88	0.02	3.91	0.01
0-degree ply	FEM	-83.63	-0.72	-0.03	3.92	0.38
	VABS	-82.57	-0.89	0.00	3.82	0.00

From Table - 5.10, it is seen that VABS and GEBT combination gives reasonable stress results for the geometrically nonlinear case when compared with the nonlinear FE solution.

5.3.6 Linear Transient Analysis of the Composite Blade (ramp load case)

In this section, the linear transient load response of the composite blade model is investigated. In the transient analysis of the composite blade, two different time varying forces are applied at the tip from the shear center. In the first load case, force increases linearly with time, stays constant for a while and then decreases again linearly until

zero, as shown in Figure - 5.14.

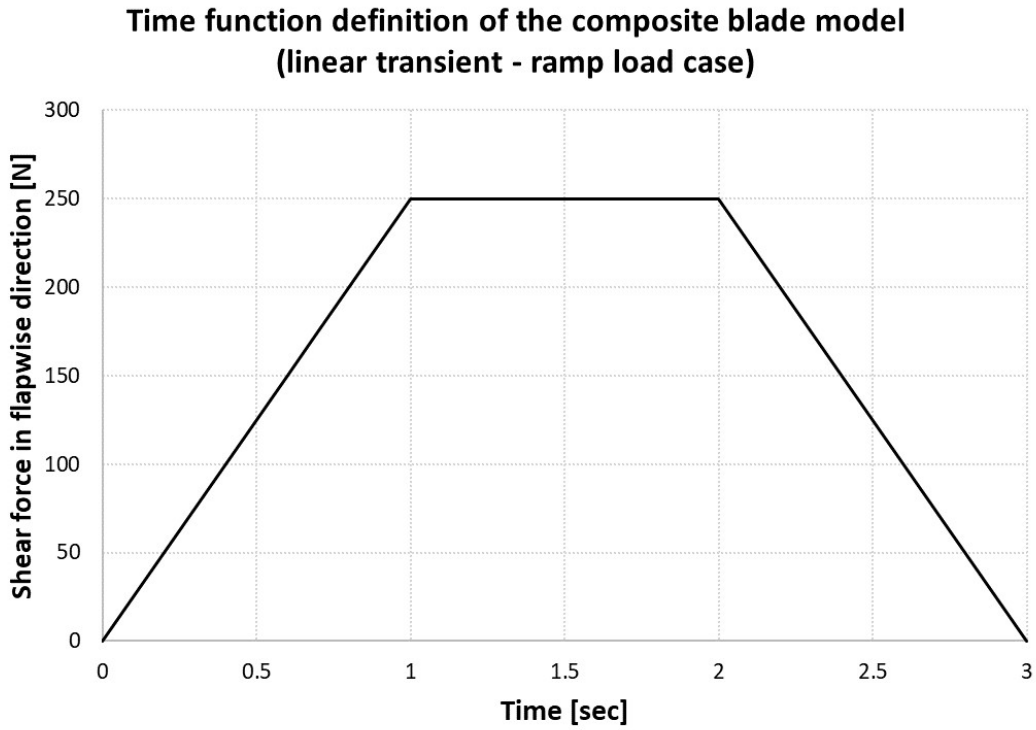

Figure 5.14: Time function definition of the composite blade model (linear transient - ramp load case).

Under this load definition, the variation of the tip displacement in flapwise direction with respect to time obtained by both finite element and GEBT analyses is shown in Figure - 5.15.

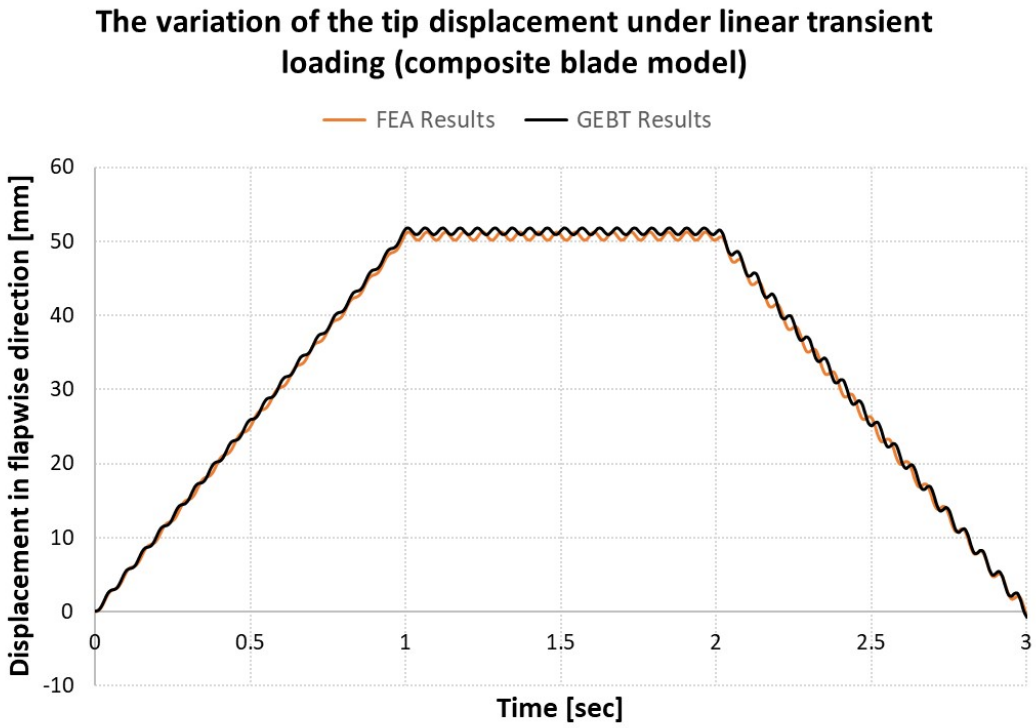

Figure 5.15: The change in the displacement in flapwise direction of the tip obtained by the FE and GEBT analysis of the composite blade.

For the linear transient load case, time responses of the tip displacement obtained by FE and GEBT analyses agree very well, as seen in Figure - 5.15.

5.3.7 Linear Transient Analysis of the Composite Blade (sine load case)

The second load definition for the transient analysis is determined given by equation-5.1.

$$F = Amplitude \cdot e^{-at} \cdot \sin(wt) \tag{5.1}$$

where $Amplitude$ is chosen as the load applied in the static analysis of the same model, which is $250[N]$. Frequency of the load variation is same as the 1^{st} bending mode of the composite blade which results in $19.32[Hz]$ from Table - 5.3; therefore, w can be calculated as $w = 2\pi f = 121.39[rad/sec]$. If '$a$' is selected as 0.5, the resultant time function of the flapwise shear force is visualized as shown in Figure - 5.16. Under this load, the flapwise tip displacement variation with time at the load application point for the FE and GEBT analyses are given in Figure - 5.17.

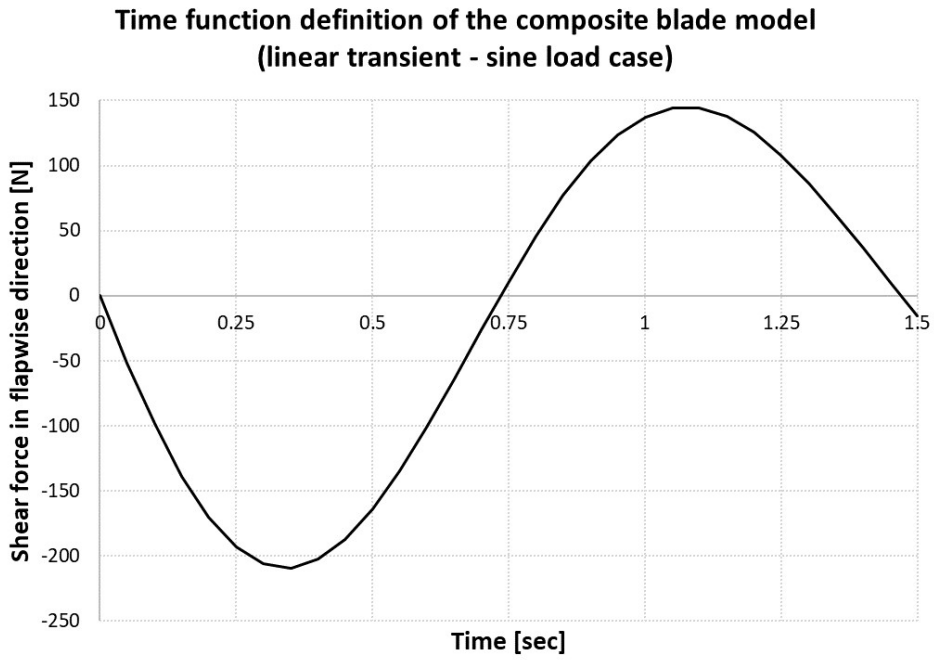

Figure 5.16: 1-cycle sine load definition in transient analysis (composite blade model).

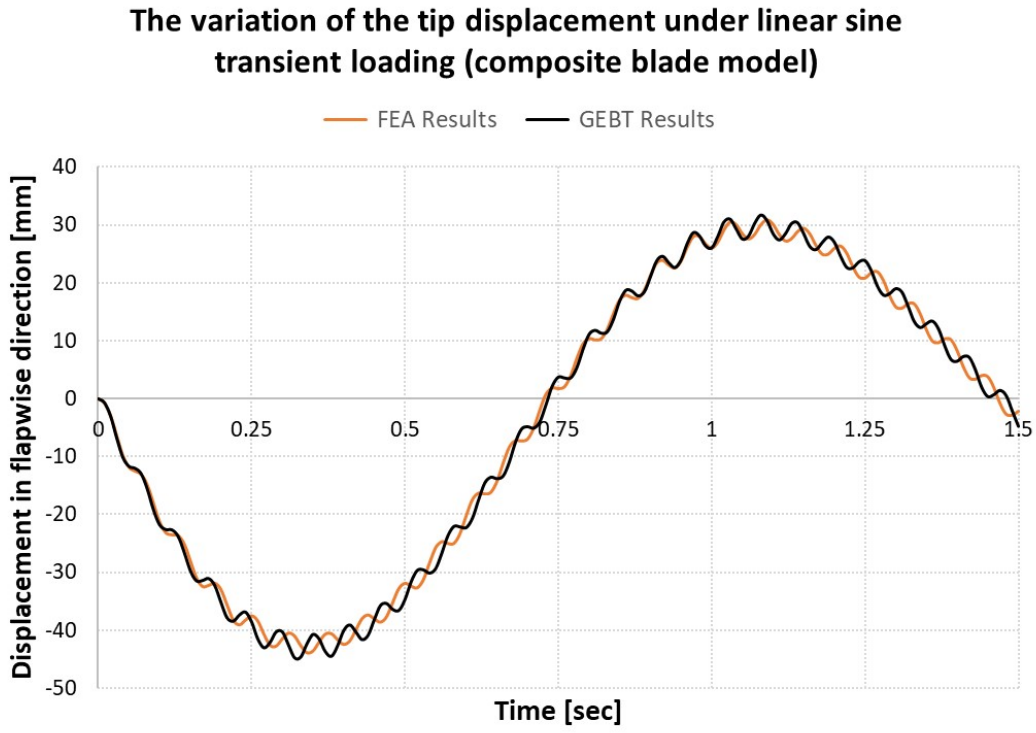

Figure 5.17: The change in the flapwise displacement of the tip obtained by FE and GEBT analysis of the composite blade model under 1-cycle sine load.

From Figure - 5.17, it is seen that the linear transient analysis displacement results obtained by the FE and GEBT analyses show that geometrically exact beam theory gives promising results when compared to the finite element method.

5.3.8 Nonlinear Transient Analysis of the Composite Blade

In the nonlinear transient analysis, the load used in the nonlinear static analysis ($500[N]$) is applied to the blade model. In MSC. Nastran, SOL129[20] is used as a solver for the nonlinear transient analysis of finite element model.
As in the linear case, the applied force increases linearly with time, stays constant for a while and then decreases again linearly until zero, as shown in Figure - 5.18. Under this load definition, Figure - 5.19 shows the variation of the tip displacement with respect to time obtained by the nonlinear transient FE and GEBT analyses.

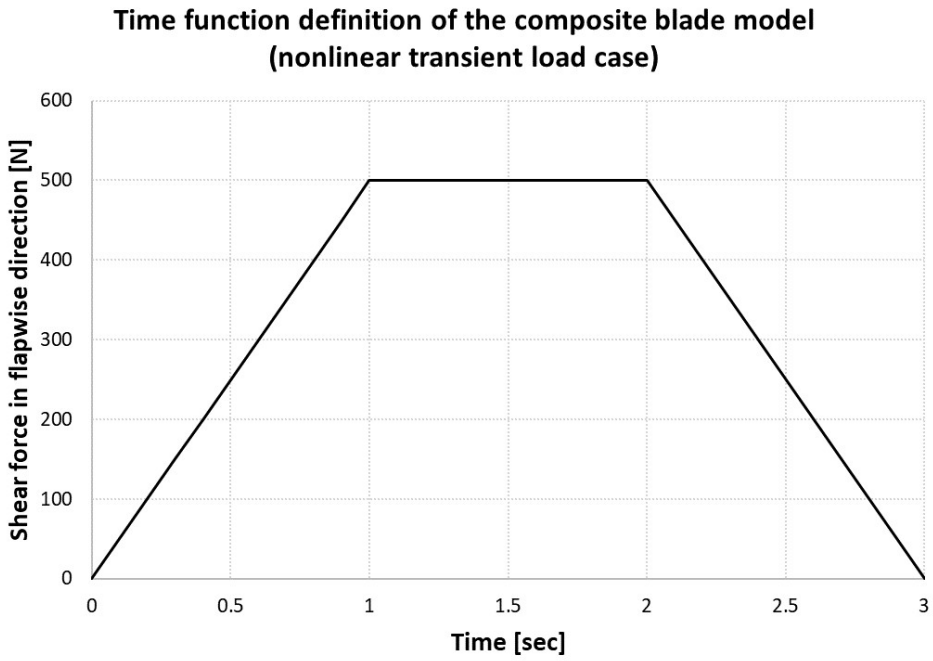

Figure 5.18: Time function definition of the composite blade (Nonlinear transient analysis).

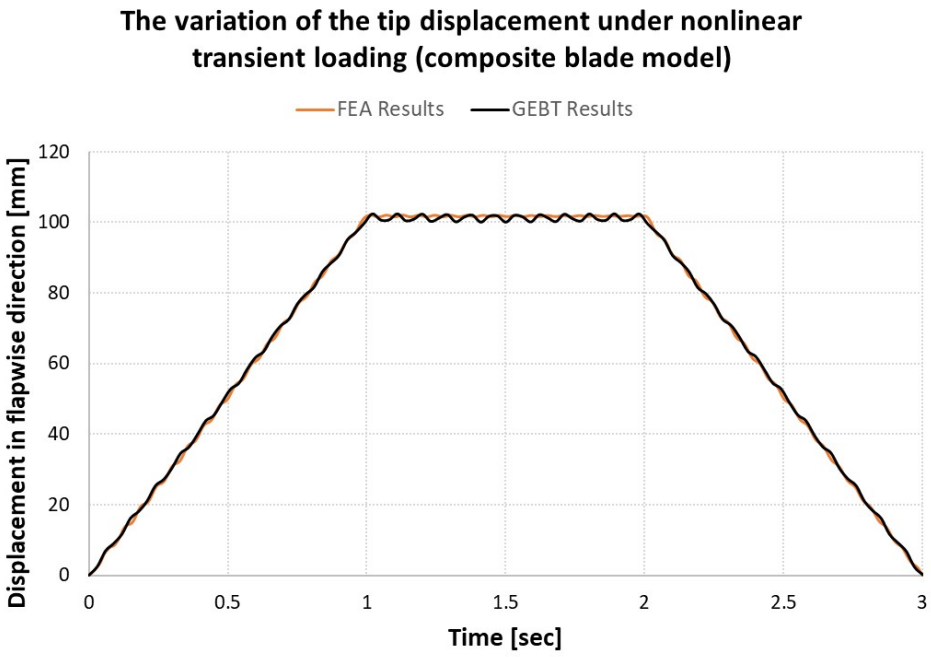

Figure 5.19: The change in the tip displacement in the flapwise direction obtained by FE and GEBT analysis of the composite blade (Nonlinear transient analysis).

From Figure - 5.19, it is seen that the nonlinear transient analysis responses of FE and GEBT analyses are in good agreement with each other. Thus, it can be said that GEBT gives promising results compared to the FEA under the nonlinear transient load case, too.

As pointed out before, in time marching aeroelastic analysis of the blade, the use of the GEBT model would substantially reduce the computational cost while still keeping the accuracy almost same as the 3D finite element based analysis.

CHAPTER 6

CONCLUSIONS AND DISCUSSIONS

This thesis presents the comparative study of the finite element analysis and the geometrically exact beam analysis of a slender composite helicopter tail rotor blade. The geometrically exact beam analysis handles all geometric nonlinearities due to large displacements and rotations of the beam problem that obeys the small strain assumptions. The lessons learned and the future aspects are discussed in this chapter.

In this master thesis, the applicability of cross-sectional analysis in the early design stages of the composite helicopter blade is investigated. For this purpose, different kind of analyses are performed for different models. The models that are chosen, from the simplest to complex, are the rectangular cross-sectional, Aluminum airfoil profile and the composite helicopter blade model. After creating the cross-sectional and the detailed finite element models, the results of the modal, linear and nonlinear static, linear and nonlinear transient analyses are collected.

For the finite element analyses, MSC. Patran[20] and MSC. Nastran[20] are used as the pre and post processors. And for the cross-sectional analyses, PreVABS[3] is used to generate the finite element mesh of the airfoil profiles. VABS (Variational Asymptotic Beam Section analysis)[1] is utilized to calculate the sectional properties; like stiffness and mass matrices, location of the neutral axis and shear center and to perform stress recovery analyses. GEBT (Geometrically Exact Beam Analysis)[2] is used to determine the sectional loads and global behavior of the beam; in other words, displacements and rotations along the span of the beam.

From the results of the analyses, it is seen that the neutral axis, shear center, still

air natural frequency, static and transient displacement and static stress analysis results of the cross-sectional analysis tools, VABS and GEBT together, match well with the FEM results for the rectangular section and airfoil section blade models studied. Thus, it is concluded that the geometrically exact beam analysis can be utilized in the early design stage of the slender structures, that can be modeled as a beam, in order to save time at this stage of the design. By this way, the computational time can be decreased significantly by keeping the accuracy of the analyses when compared to the finite element analyses. It is deemed that in the regions away from the blade root where three dimensional effects are not significant, high accuracy of the combination of the geometrically exact beam method and the variational asymptotic beam section method allows this methodology to be used in the detailed design phase. However, in the vicinity of the boundaries, or where the mesh quality is not good in the cross-sectional analyses, the finite element analysis should be performed. It is considered that combination of finite element approach and 1D beam and cross-sectional analysis methods can be utilized for the design and analysis of the whole helicopter blade in the detailed design phase.

By presenting comparison studies between the finite element and the cross-sectional analysis, for the region away enough to the boundary, it is concluded that using VABS and GEBT together provides accurate solutions for the static and dynamic analysis of the blade. It is considered that especially for the structural design of the airfoil sections of the blade, which requires many re-analyses due to frequent design changes in the detailed design stage, geometrically exact beam analysis can replace finite element method which requires longer modelling times to reflect the design changes.

With this study, the applicability of the geometrically exact beam analysis on the helicopter blade is shown and it is aimed to increase the use of this methodology in the design of slender blade structures since the low computational analysis time required by the cross-sectional analysis over the finite element solution time is a major advantage.

As future studies, the time marching aeroelastic analyses and optimization studies which require repeated analyses can be performed by VABS-GEBT combination. In

the case of aeroelastic analysis, by coupling the VABS-GEBT combination with an aerodynamic solver, static and dynamic aeroelastic problems can be solved and comparisons can be performed with the finite element based aeroelastic analysis. It is deemed that the real advantage of using the reduced order but high fidelity model of blades, such as the VABS-GEBT combination, can be understood better in problems which require repeated analysis. Such studies are the potential future work that have to be performed pursuing this study.

REFERENCES

[1] Yu W. Vabs manual for users. Technical report, Utah State University Technology Commercialization Office and Georgia Institute of Technology Research Cooperation, 13 February 2013.

[2] Yu W. Manual of gebt. Technical report, Utah State University, 26 October 2011.

[3] Chen H. and Yu W. Manual of prevabs. Technical report, Utah State University, 8 December 2008.

[4] Cesnik C. E. S. and Hodges D. H. A new concept for composite rotor blade cross-sectional modeling. 1995.

[5] Damiani R., Jonkman J., Robertson A. and Song H. Assessing the importance of nonlinearities in the development of a substructure model for the wind turbine cae tool fast. In *32nd International Conference on Ocean, Offshore and Arctic Engineering*, March, 2013.

[6] Chen H., Yu W. and Capellaro M. A critical assessment of computer tools for calculating composite wind turbine blade properties. *Wind Energy*, 13(6):497–516, 2009.

[7] Giavotto V., Borri M., Mantegazza P., Ghiringhelli G.L., Caramaschi V., Maffioli G.C. and Mussi F. Anisotropic beam theory and applications. *Computer and Structures*, 16:403–413, 1983.

[8] Wang Q., Yu W. and Sprague M. A. Geometric nonlinear analysis of composite beams using wiener-milenkovic parameters. In *54th /ASME/ASCE/AHS/ASC Structures, Structural Dynamics, and Materials Conference*, 2013.

[9] Yu W., Hodges D. H., Volovoi V. V. and Fuchs E. D. A generalized vlasov theory for composite beams. *Thin Walled Structures*, 43(9):1493–1511, 2005.

[10] Yu W. and Hodges D. H. Generalized timoshenko theory of the variational asymptotic beam sectional analysis. *Journal of the American Helicopter Society*, 10:46–55, 2005.

[11] Yu W. and Blair M. Gebt: A general-purpose nonlinear analysis tool for composite beams. *Composite Structures*, 94(9):2677–2689, 2012.

[12] Hodges D. H., Shang X. and Cesnik C. E. S. Finite element solution of nonlinear intrinsic equations for curved composite beams. In *36th Structures, Structural Dynamics and Materials Conference*, 1996.

[13] Epps J. J. and Chandra R. The natural frequencies of rotating composite beams with tip sweep. *Journal of the American Helicopter Society*, 41(1):29–36, 1996.

[14] Yu W. *Variational Asymptotic Modeling of Composite Dimensionally Reducible Structures*. Phd, Georgia Institute of Technology, July 2002.

[15] Hodges D. H. *Nonlinear Composite Beam Theory*. American Institute of Aeronautics and Astronautics, Inc., 2006.

[16] Bauchau O. Computational schemes for flexible, nonlinear multi-body systems. *Multibody System Dynamics*, 2:169–225, 1998.

[17] Yu W. and Blair M. A general-purpose implementation of the mixed formulation of the geometrical exact beam theory. In *51st AIAA/ASME/ASCE/AHS/ASC Structures, Structural Dynamics, and Materials Conference*, 2010.

[18] Gunel M. and Kayran A. Non-linear progressive failure analysis of open-hole composite laminates under combined loading. *Journal of Sandwich Structures and Materials*, 15(3):309–339, 2013.

[19] *MSC Nastran 2012 Linear Static Analysis User's Guide*. MSC Software, 2011.

[20] *MSC Patran Nastran Preference Guide, Vol. 1: Structural Analysis*. MSC Software, 2005.

APPENDIX A

EXAMPLE OF VABS AND GEBT INPUT FILES

A.1 Example of VABS Input File

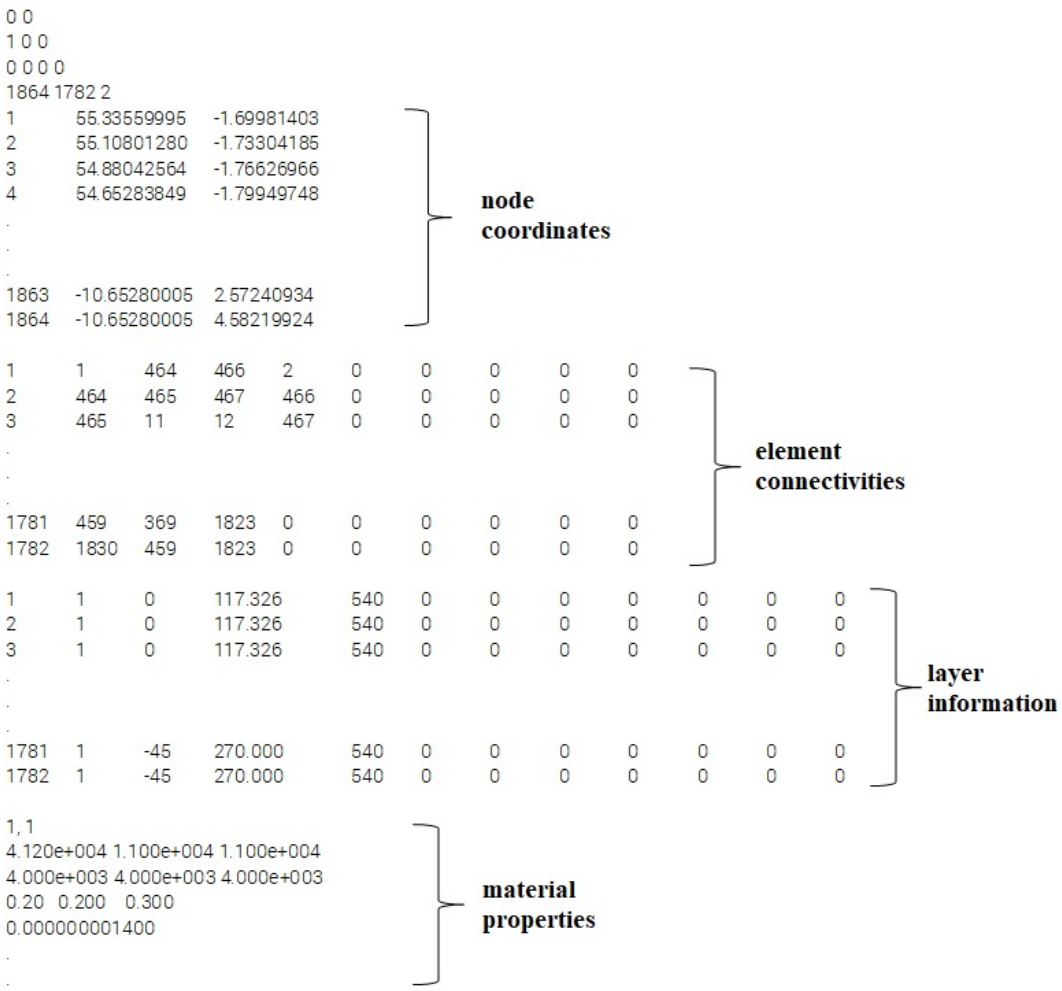

Figure A.1: Example of VABS input file.

A.2 Example of GEBT Input File

```
0 1 100 # analysis control parameters

2   1  2 1 0  0 0 1 0  # information of the members and the key points

1    0.0      0.0    0.0   # coordinates of the points
2    900.0  0.0    0.0

1    1     2  1  1  0 180  0  # information about the members like the number of elements, cross-
section, etc.

1    #point conditions
1 2 3 4 5 6
0 0 0 0 0 0 # corresponding value
0 0 0 0 0 0 # corresponding time functions
0 0 0 0 0 0 # indicate whether it is a follower condition

2
7   8  9  10 11 12
1e5 0  0  0  0  0
1   0  0  0  0  0
0   0  0  0  0  0

1 # section No. 1 Flexibility Matrix
   4.223089E-08      .         .         .         .         .
                     .         .         .         .         .
                     .         .         .         .         .
                     .         .         .         .         .
                     .         .         .         .         .
                     .         .         .         .  1.757096E-11

0 1 # simulation range
1   # time function no
0
0 1
2   # number of entries
0 0
1 1
```

Point conditions of prescribed displacements, rotations, forces, or moments.

Flexibility Matrix (6x6)

Time Function

Figure A.2: Example of GEBT input file.